


Spring 4-14-2018

Evaluating the Aryl Hydrocarbon Receptor as a Target for Pharmacologic Activity of Repurposed Drugs

Teofilo Borunda Duque

Follow this and additional works at: https://digitalrepository.unm.edu/phrm_etds

 Part of the [Medicinal Chemistry and Pharmaceutics Commons](#), [Other Chemicals and Drugs Commons](#), [Pharmacology Commons](#), and the [Toxicology Commons](#)

Recommended Citation

Borunda Duque, Teofilo. "Evaluating the Aryl Hydrocarbon Receptor as a Target for Pharmacologic Activity of Repurposed Drugs." (2018). https://digitalrepository.unm.edu/phrm_etds/19

This Thesis is brought to you for free and open access by the Electronic Theses and Dissertations at UNM Digital Repository. It has been accepted for inclusion in Pharmaceutical Sciences ETDs by an authorized administrator of UNM Digital Repository. For more information, please contact disc@unm.edu.

Teofilo Borunda
Candidate

Graduate Unit Pharmaceutical Sciences
Department

This thesis is approved, and it is acceptable in quality and form for publication:

Approved by the Thesis Committee:

Todd Anthony Thompson, Chairperson

Tudor Oprea

Graham S Timmins

Prashant Nighot

**Evaluating the Aryl Hydrocarbon Receptor as a Target for
Pharmacologic Activity of Repurposed Drugs**

BY

Teofilo Borunda Duque

B.A., Chemistry, New Mexico State University, 2014

THESIS

Submitted in Partial Fulfillment of the
Requirements for the Degree of

**Master of Science
Pharmaceutical Sciences**

**Department of Pharmaceutical Sciences
Department of Biochemistry and Molecular Biology**

The University of New Mexico

Albuquerque, New Mexico

May 2018

DEDICATION

I dedicate this work in loving memory of my grandfather Teofilo Borunda Flores as my admiration for his hard work and achievements have acted as a fuel for my career growth and development. His legacy ultimately allowed me to pursue my dreams to become a medical scientist for which I will be eternally grateful.

ACKNOWLEDGEMENTS

Completing this thesis while in pharmacy school has been without a doubt one of the hardest things I have ever accomplished academically until now. However, now that it is finished it is wonderful to look back at the extraordinary group of people who helped me accomplish such a big task. I would like to begin by thanking my committee members and mentors Dr. Tudor Oprea, Dr. Graham Timmins, Dr. Prashant Nighot, Debra MacKenzie and particularly Dr. Thompson who, despite my lack of enthusiasm about soccer or star trek, still took me under his wing and mentored me through pharmacy and graduate school. The mentorship of Dr. Thompson really helped me discover a new potential I did not know I had. His guidance, support, and encouragement played a big role in the inception and completion of this project for which I will always be grateful.

To my family, particularly my loving parents Teofilo Borunda and Patricia Duque who gave me the opportunity to pursue my dreams, my siblings Ricardo Chretin, Rodrigo Borunda, Patricia Borunda whose love and support always helped me move forward. My cousin Marco Borunda who would call me often to check on my progress and motivated me to keep moving forward. My brother-in-law, Rallin Harris, who made sure I was well fed by cooking and bringing food to our house when we were too busy to cook.

Above all, I would like to thank my wife, Jaryse Harris, who throughout pharmacy and graduate school attended and assisted with every single poster session, seminar, and project in which I participated. Her love and constant support helped keep me sane and optimistic when I was overwhelmed, energized when I was tired, and focused when I was distracted. Thank you for always being there for me and for being my editor, my practice audience, my sounding board, and my best friend. But most of all, thank you for being by my side every single step of the way. I am very fortunate to have you in my life and to be able to share this new accomplishment with you.

**EVALUATING THE ARYL HYDROCARBON RECEPTOR
AS A TARGET FOR PHARMACOLOGIC ACTIVITY OF REPURPOSED
DRUGS**

By

TEOFILO BORUNDA DUQUE

B.A., CHEMISTRY, NEW MEXICO STATE UNIVERSITY, 2014

**MASTER OF SCIENCES
PHARMACEUTICAL SCIENCES**

ABSTRACT

The discovery of new pharmacologic targets is important for the advancement of pharmacotherapy and identification of new indications for current drugs. The aryl hydrocarbon receptor (AHR) is a physiologic sensor of both chemical environmental pollutants and ligands of natural origin. Given the broad spectrum of ligands that activate the AHR and its relationship with toxicology, the AHR is not thought to be a traditional target for pharmacotherapy. However, multiple studies have shown potential for the AHR as a novel pharmacologic target. Therefore, identifying less toxic agents that modulate the AHR may elucidate mechanisms for pharmacological targeting of the AHR. The hypothesis addressed for this thesis project is that *chemical libraries of established drugs can be used to map the pharmacological space of the aryl hydrocarbon receptor*. Three specific aims are proposed to address this hypothesis. Specific aim 1: Develop a high

throughput screening assay to identify established drugs that activate the AHR. Specific aim 2: Use a chemical library of known pharmacologically active agents to map pharmacological space of the AHR and identify a lead compound for further evaluation. Specific aim 3: Determine chemical structure activity relationship of the lead compound's pharmacophores and AHR activation potency. The AHR assay developed for Aim 1 incorporated an AHR-responsive green fluorescence protein (GFP) reporter that could be transduced into any cell type of interest. For normalization of transduction efficiency, a dtTomato expressing vector was optimized for expression without interference of the GFP reporter. Both the human colon cancer cell line Caco2 and the liver cancer cell line HepG2 were used in these studies. Drug screening for AHR activation using the AHR assay resulted in the identification multiple ligands including a lead compound. The lead compound in this study used for further evaluation was alpha-tocopherylquinone (TQ). The quinone structure is a critical component of TQ, interestingly other AHR ligands have been found to have a quinone structure as a molecular component. (eg dioxin) However, quinone structure ability to activate the AHR is less defined compared to other compounds like polycyclic carbons. In this study, differences were observed in the toxicity and AHR activation profile of fully substituted and unsubstituted para-quinones. The findings from these experiments suggest that there is a direct relationship between the number of carbon substitutions and the potency of the para-quinone to elicit an effect on the AHR. For example, we found that benzoquinone (BQ), an unsubstituted para-quinone was a relatively potent ligand of the AHR. Furthermore, adding a single methyl group to the benzoquinone increased its potency to activate the AHR. However, further methyl substitutions to the para-quinone ring diminished the para-quinone potency to activate the AHR. A compound

that supported this observation was duroquinone, a fully substituted para-quinone which showed no AHR activity in the AHR assay. This study identifies critical characteristics necessary for para-quinones to activate the AHR and gives rise to a new class of compounds with potential of becoming novel treatments for disease through AHR activation.

TABLE OF CONTENTS

DEDICATION	iii
ACKNOWLEDGEMENTS	iv
ABSTRACT	v
CHAPTER 1: INTRODUCTION	1
Introduction Summary	2
Aryl Hydrocarbon Receptor Biology	4
Aryl Hydrocarbon Receptor Background and Function	5
The Role of Aryl Hydrocarbon Receptor in Inflammatory Pathways	7
Potential of the Aryl Hydrocarbon Receptor as a Pharmacologic Target	8
Drug Repurposing	10
Quinones	11
Background Research from the Thompson Laboratory	13
Rationale for Investigating Quinones	16
Thesis Objectives:	18
References	19
CHAPTER 2: DIFFERENTIAL ARYL HYDROCARBON RECEPTOR ACTIVATION BY SUBSTITUTED QUINONES	21
Abstract	22
Introduction	23
Materials and Methods	25
Chemicals	25
Expression Vectors	26
Cell Culture and Transfection	26
EGFP Reporter Assay Validation	27
Cell Growth and Viability Analyses	28
Microscopic Analyses and AHRA Quantification	28
Statistical Analyses	28
Results	29

Aryl Hydrocarbon Receptor Activation Assay	29
Prestwick Library Analysis	31
Quinone Structure Analysis	34
Discussion	43
References	45
CHAPTER 3: CONCLUSIONS AND FUTURE STUDIES	48
Conclusion	49
Future Directions	49
Validation Studies	49
Future Studies	51
References	55
APPENDICES	56
Appendix 1: Modulation of autophagic flux and cell death by the antihistamine astemizole in human prostate cancer cells	57
Abstract	58
Introduction	59
Materials and Methods	61
Results	65
Discussion	68
References	71
Figure Legends	78

CHAPTER 1: INTRODUCTION

Introduction Summary

The process of drug discovery and development often starts with the identification of a target that has an association or contribution to disease progression; such as a gene, a protein, or a receptor (Li and Corey, 2013). After target identification, it is important to assess whether or not modulating the target has a therapeutic effect. Equally important, is the identification of modulators for the target and evaluation of the characteristics linked with the modulators potency. Given that the outcome of modulating the target with a less toxic agent is therapeutic, the target can then serve as a pharmacological target with the potential to treat disease. The discovery of new pharmacologic targets is important for the advancement of pharmacotherapies with novel mechanisms of action. Discovering new pharmacologic targets becomes especially important in diseases with a broad involvement of different proteins, physiological pathways and signaling such as immune mediated inflammatory diseases.

The Aryl Hydrocarbon Receptor (AHR) is an emerging target which shows promise in becoming a pharmacologic target for treating disease. The AHR for many years was extensively studied by the toxicology field for its major role in mediating the responses to a broad scope of xenobiotics and environmental pollutants such as polycyclic aromatic hydrocarbons and polychlorinated biphenyls. Nonetheless, the AHR has recently enticed the attention of immunologists due to its extensive expression in the immune system and its involvement in important physiological pathways such as inflammation (Stockinger et al., 2014). AHR involvement in inflammation, has illustrated the potential for the AHR as a novel pharmacological target for the treatment of diseases with inflammatory pathways, e.g. inflammatory bowel disease.

The AHR may be a feasible target for the treatment of inflammation in inflammatory bowel disease because it may provide more selective treatment with less side effects compared to the anti-inflammatory methods currently employed to treat inflammatory bowel disease (Ehrlich and Kerkvliet, 2017). However, there are several factors complicating the pharmacological considerations for the AHR. For example, there are many different ligands known to activate the AHR. That is, the AHR can be activated by a wide array of chemically diverse structures. Since activation of the AHR is mediated by many different ligands, it is challenging to precisely understand the structure and chemical properties required for AHR ligands. Another factor that complicates pharmacological considerations of the AHR is the fact that most AHR ligands studied to date are toxins, and they do not possess acceptable characteristics as pharmaceutically acceptable targets. Hence, the AHR historically has been considered important as a mediator toxicological action. Based on these considerations, an area of interest addressed in this thesis is to elucidate characteristics necessary for less toxic chemical functional groups to activate the AHR.

In the interest of finding less toxic chemical functional groups to act as AHR ligands, a drug screening assay of an augmented version of the Prestwick Chemical Library was developed (It was an augmented version of the Prestwick Library due to the inclusion of para-quinones). This presented a very attractive opportunity since the AHR appears to have low selectivity for ligands. Hence, it was expected for the AHR to have multiple unknown ligands already on the market. Furthermore, the drugs used in these efforts have already proven to be effective in pharmacological action; safe and extensive information is available based on their prior use. Following the results of the augmented Prestwick library

screening, a group of compounds was chosen for further evaluation of the functional groups responsible for each compound's potency.

A few "hits" were identified resulting from the drug screening including quinones, which we decided to focus further studies. Due to the fact that they are derivatives of aromatic compounds which are seen extensively in pharmaceutical drugs and their activity to modulate the AHR has not been profoundly investigated. The results from the studies completed in this thesis may provide better understanding of the ligands that activate the AHR and the chemical characteristics required in quinone structures to modulate their potency to activate the AHR.

Aryl Hydrocarbon Receptor Biology

The AHR is a ligand activated transcription factor, a member of the basic helix-loop-helix (bHLH-PAS) transcription factors, and is expressed broadly in the body. For example, the AHR without the presence of a ligand is present in the cytoplasm bound to actin filaments as an inactive complex with several chaperone proteins, including HSP90, AIP, and p23 (Stockinger et al., 2014). When a ligand binds to the AHR, the complex detaches from the actin filament and translocates into the nucleus, where it is released from the complex, heterodimerizes with the aryl hydrocarbon receptor nuclear translocator protein (ARNT; a.k.a. HIF-1beta) and then binds to the region of the genome containing its binding motif, the dioxin response element (DRE), also referred to as the xenobiotic response element (XRE). After the AHR:ARNT complex binds to the DRE, it modulates the transcription of genes such as CYP1A1, CYP1A2, CYP1B1, and the AHR repressor (AHRR). The signaling of the AHR is regulated at three levels: AHR protein degradation,

ligand metabolism by CYP1A1, and disruption of the AHR/ARNT complex by AhRR. (Stockinger et al., 2014).

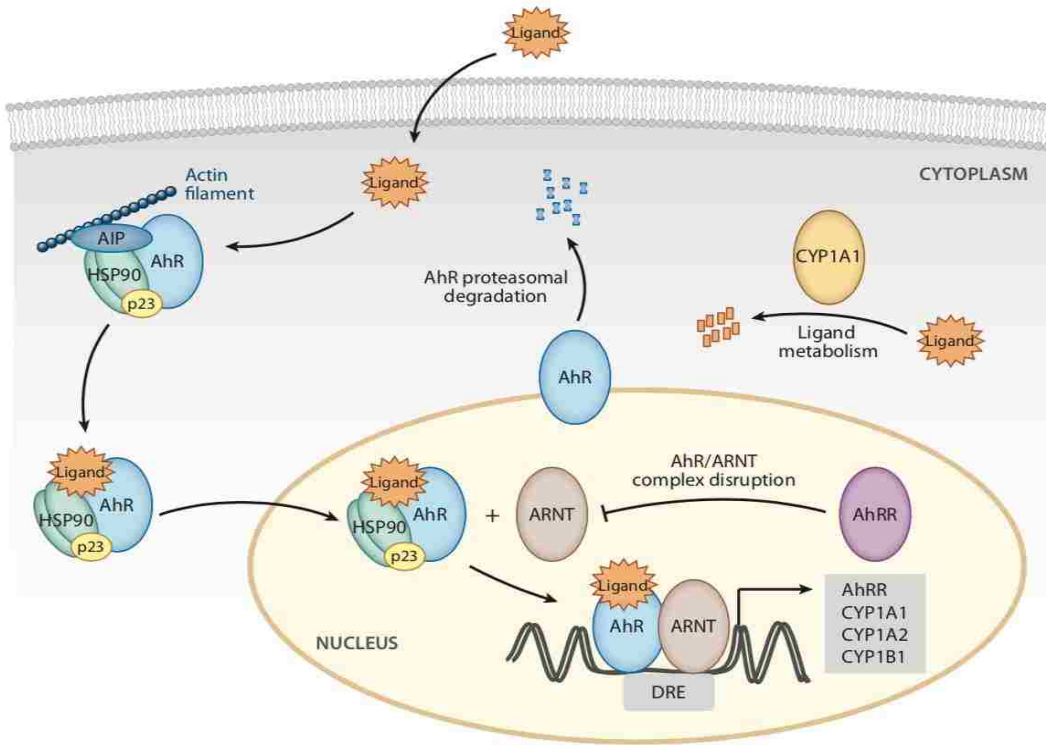


Figure 1. Illustration of the mechanism of ligand activated aryl hydrocarbon receptor activation (from Stockinger et al., 2014).

Aryl Hydrocarbon Receptor Background and Function

The AHR was first discovered and investigated because of its recognition as mediator of the toxicity of 2,3,7,8-tetrachlorodibenzodioxin (TCDD) (Stockinger et al., 2014). TCDD is a chemical produced as a side product of industrial organic synthesis of herbicides as well as used as a defoliant in the Vietnam War, known as the Agent Orange. It was also responsible for toxicities associated with the Seveso disaster in Milan, Italy in 1976. The Seveso disaster was an industrial accident that resulted in the highest known

exposure of TCDD in residential populations, which gave rise to numerous scientific studies and standardized industrial safety regulations (Pesatori et al., 2003). TCDD was found to cause chloracne in addition to life-threatening clinical complications such as progressive liver failure, emphysema, renal failure, and myocardial degeneration (Stockinger et al., 2014)

Ongoing research revealed that the AHR was not a specific receptor for TCDD. As a matter of fact, AHR mediates many responses to a broad scope of xenobiotics and environmental pollutants, such as polycyclic aromatic hydrocarbons and polychlorinated biphenyls (Vondracek et al., 2004). These environmental pollutants promote a number of toxic and carcinogenic responses in animals and humans when they activate the AHR. Activation of the AHR upregulates the transcription of many detoxification genes, including those coding for the Phase I xenobiotic-metabolizing cytochrome P450 enzymes CYP1A1, CYP1A2, CYP1B1, and CYP2S1, and the phase II enzymes UDP-glucuronosyl transferase UGT1A6, NAD(P)H-dependent quinone, oxydoreductase-1 NQO1, the aldehyde dehydrogenase ALDH3A1, and several glutathione-S-transferases (Vondracek et al., 2004).

Conversely, evidence from AHR knockout mice reveals that the AHR has functions independent of toxicity and detoxification of harmful xenobiotics. Absence of the AHR in AHR-null mice gives rise to cardiovascular disease, hepatic fibrosis, reduced liver size, spleen T-cell deficiency, dermal fibrosis, liver retinoid accumulation and shortening of life span (Puga et al., 2010). Likewise, there have been multiple studies that have specifically studied the involvement of the AHR with different physiological responses, including inflammatory pathways (Murray et al., 2017), (Benson and Shepherd, 2011), (Wang et al.,

2017). Owing to the involvement of the AHR with many different physiological responses as seen by these studies, the AHR becomes an attractive and innovative target for the advancement of pharmacotherapy.

The Role of Aryl Hydrocarbon Receptor in Inflammatory Pathways

Activation of the AHR has been linked with either enhancement or repression of inflammatory signaling. However, in the gastrointestinal tract, most studies support that the activation of the AHR by a ligand produces an anti-inflammatory outcome (Murray et al., 2017). One of the studies that furthers explores this concept is the study published by Jenna M. Benson and David M. Shepherd from the University of Montana (Benson and Shepherd, 2011). In their study, it was found that AHR activation by TCDD reduced the inflammation associated with Crohn's disease. Mice were gavaged with TCDD prior to presensitization and colitis induction. After TCDD exposure, colitis was induced via an intrarectal instillation of 2,4,6-trinitrobenzenesulfonic acid (TNBS). Following TCDD exposure and colitis induction, body weight loss and the severity of clinical symptoms was evaluated (overall body condition, stool consistency, and dehydration state via a skin pinch test) and the severity of each clinical sign was also scored. These investigators observed that mice without TCDD exposure lost approximately 17% of their initial body weight following TNBS exposure and did not recover by the end of the study. In contrast, TCDD-exposed mice lost only 8% of their initial weights and recovered weight rapidly.

Also, a protective effect of TCDD in the clinical severity of colitis was observed, as seen by stool consistency, dehydration, and body condition. Lastly, Benson and Shepherd (2011) looked at the difference in inflammation between the mice and the difference in gene expression in order to assess if there was a correlation between the AHR

and TCDD mediated improvement of colitis. Inflammation was significantly reduced in the mice treated with TCDD. With respect to gene expression, they reported an upregulation in the expression of Cyp1A1, which was a significant finding in their study as CYP1A1 is a well-established marker of AHR activation. An additional study that illustrates the use of the AHR as a pharmacologic target for the treatment of gastrointestinal inflammation was published by Wang and Yang (2017). In this study, the potential of the AHR to attenuate colon inflammation in mice was investigated. To accomplish this, a group of mice that expressed the AHR and another group of mice with an AHR knockout were used. Colitis was induced in both mouse groups by administering 3% dextran sulfate sodium (DSS) for 7 days. Both groups were also administered 6-formylindolo(3,2-b) carbazole (FICZ), a well-established activator of the AHR (Jönsson et al., 2009); starting 2 days after the administration of DSS. The results from this study indicated that the injection of mice with FICZ in the AHR group significantly attenuated DSS-induced colitis and decreased the expression levels of inflammatory cytokines and AHR expression was upregulated. In addition, the mice with the AHR knockout exhibited elevated inflammatory cytokine production and developed more severe colitis. (Wang et al., 2017). The findings from both the Benson and Wang studies further support the AHR as a pharmacological target for the treatment of disease, at least for inflammatory pathways such as inflammatory bowel disease.

Potential of the Aryl Hydrocarbon Receptor as a Pharmacologic Target

Studies examining the relationship between the AHR and the immune system have identified unique characteristics that may improve the safety profile when compared with other immunosuppressant drugs. Given the fact that memory responses are less sensitive

to immune suppression by AHR activation than primary immune responses suggests that activating the AHR by a ligand may not interfere with the established immunity. (Ehrlich and Kerkvliet, 2017). These findings, in conjunction with the attenuation of inflammation in colitis after AHR activation seen in the gastrointestinal studies of Benson and Wang increases the likelihood of the AHR for use as a target for pharmacotherapy; as these findings highlight the therapeutic effect following AHR activation. Given the connection between the AHR and toxic pollutants, it is thought that activators of the AHR are toxic, which gives rise to hesitation regarding the use of ligands to activate the AHR for pharmacotherapy. Therefore, it is crucial to expand our knowledge of AHR ligands as well as their toxicity in order to be able to use the AHR as a pharmacologic target.

In an effort to increase our understanding of AHR ligands and their toxicity, multiple studies have screened drugs for AHR activity and have successfully found less toxic AHR activators. A large scale screening of 596 compounds *in vivo* assessed the induction of CYP1A1 and other AHR related genes in liver, kidney, and heart (Hu et al., 2007). From the screening a subset of 147 compounds, they were then evaluated *in vitro* for their ability to activate the AHR using a combination of gel shift, reporter gene, and competitive reporter binding assays. The combination of the *in vivo* and *in vitro* studies identified nine AHR agonists of which six were marketed FDA approved drugs. The FDA approved compounds identified were flutamide, leflunomide, nimodipine, omeprazole, sulindac, and raloxifene (Hu et al., 2007). From these six drugs none of them produced dioxin-like toxicity in rats or humans. The findings from this study and others have not only shown that AHR activation does not always result in dioxin-like toxicity but also illustrates the lack of selectivity of the AHR has for ligands.

Drug Repurposing

Given the fact that the AHR is activated by many different compounds which may include currently marketed FDA-approved drugs, there is a high probability of being able to repurpose an off-patent FDA approved drug for therapeutic activation of the AHR. The concept of drug repurposing is the application of known drugs and chemical compounds to treat new indications in addition to the indications they had when they first came out to the market (Oprea et al., 2011). Drug repurposing has seen an increase in potential since there has been a reduction in the number of new drugs reaching the market due to the high costs of development and low approval odds for drugs (Oprea et al., 2016). On the other hand, the cost of repurposing drugs is significantly lower and the probability of success is higher due to the fact that the drugs have already been on the market and an extensive database for their safety, pharmacokinetics and pharmacodynamics. Besides pharmaceutical industries turning their attention to drug repurposing, academia and small business research efforts have played an increasing role in drug discovery, with drug repurposing as one of the major areas of activity (Oprea et al., 2016). As a means of repurposing drugs for AHR therapeutic activation, for this study, an AHR reporter assay was developed to screen the Prestwick library, a chemical library of 1,280 off-patent drugs.

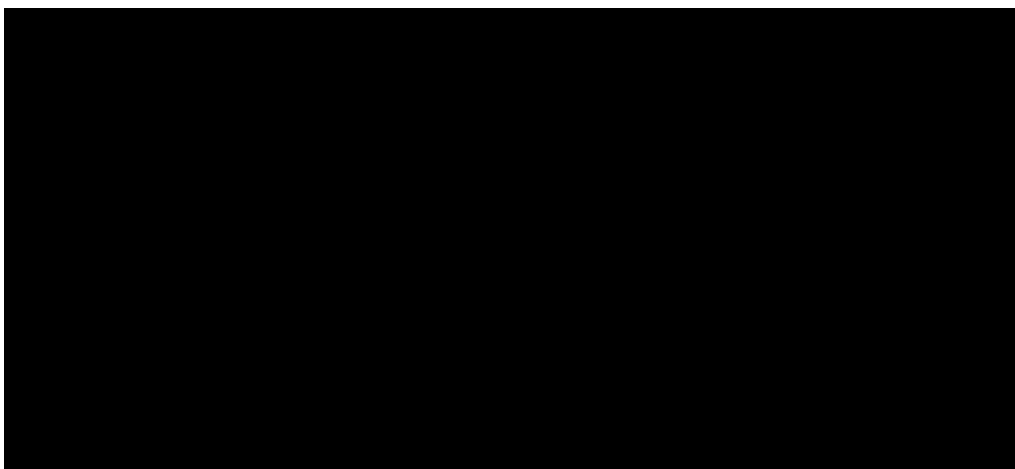
Alpha-tocopherylquinone (TQ) was identified as a lead compound for activation of the AHR with strong pharmacotherapeutic potential. TQ was a very interesting finding since it was speculated that most AHR ligands had to have a polycyclic component in their structure in order to activate the AHR. Quinone structures on the contrary have not been extensively evaluated for their use as AHR ligands. Given the novelty of these findings,

we further investigated quinone structures and their potential to become pharmacologic activators of the AHR.

Quinones

Quinones are derived from aromatic compounds, such as benzene and naphthalene, by conversion of an even number of $-CH=$ groups into $-C(=O)-$ groups with any necessary rearrangement of double bonds, resulting in a fully conjugated cyclic dione structure (Bolton et al., 2014). This quinone formation is illustrated in Figure 2.

Figure 2.






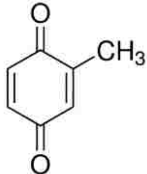
(Bolton et al., 2016)

Figure 2. Example of metabolic pathways converting aromatic compounds to quinones.

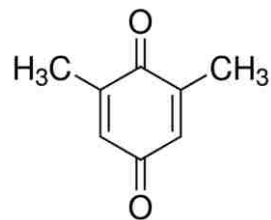
Quinone structures and derivatives are relevant in biology due to their prevalence in foods and in different biological pathways. For instance, the quinone vitamin K has been directly involved in the regulation of blood clotting. Other quinones like TQ, the oxidation product of vitamin E, has been shown to be involved in oxidation-reduction reactions (Infante et al., 1999). Additionally, flavonoids and flavonoids which are antioxidants

commonly found in foods, are also quinones. In the pursuit of elucidating the characteristics necessary for quinones to activate the AHR, 1,4 cyclohexanedione a “simple” quinone was picked and its ability to modulate the AHR was compared to quinones with the same backbone structure, but different substitutions on the carbons as seen on the following table.

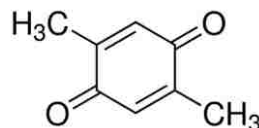
Table 1. Quinone structures investigated in this study.

	
1,4 Cyclohexanedione	
Benzoquinone	
Methyl-p-benzoquinone	

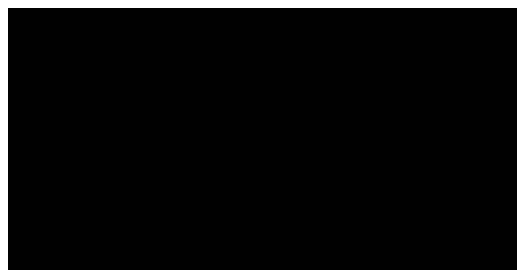
2,6-Dimethylbenzoquinone



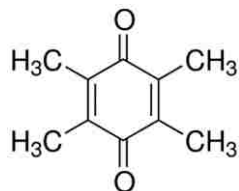
2,5-Dimethyl-1,4-benzoquinone



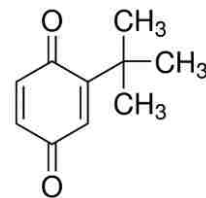
Trimethylbenzoquinone



Duroquinone



2-tert-Butyl-1,4-benzoquinone



Background Research from the Thompson Laboratory

Dr. Thompson's laboratory performed microarray studies with prostate cancer cells using Affymetrix Human Genome U1333A. Plus 2.0 GeneChip arrays to examine alterations in gene expression induced by TQ. These findings showed that a high ranked pathway modulated by TQ included xenobiotic metabolism pathways. An increase in phase

I and II metabolizing enzymes such as CYP 1A1, aldoketoreductase 1C1, AKR1B10, glutamate-cysteine ligase, and AHR expression was observed as shown in the following table.

Table 2. Messenger RNAs induced by TQ

Gene	Gene Symbol	Accession Number	[mRNA] Fold ↑
<i>Aldoketoreductase 1C1</i>	AKR1C1	NM_001353	96.0
<i>Cytochrome P450 1A1*</i>	CYP1A1	NM_000499	43.1
<i>Aldoketoreductase 1B10*</i>	AKR1B1	NM_020299	24.0
<i>Glutamate-cysteine ligase, modifier-subunit</i>	GCLM	NM_002061	4.9
<i>Aldehyde dehydrogenase 3A2*</i>	ALDH3A2	NM_000382	4.3

Additional studies performed in the Thompson laboratory observed activation of an XRE/DRE luciferase reporter with TQ, but not VE (Figure 3). Lastly she also performed experiments where she used siRNA for AHR to knockdown AHR expression in LNCaP prostate cells to see if AHR mRNA and CYP 1A1 mRNA levels were dependent to AHR activation by TQ (Figures 1b,1c, and 1d).

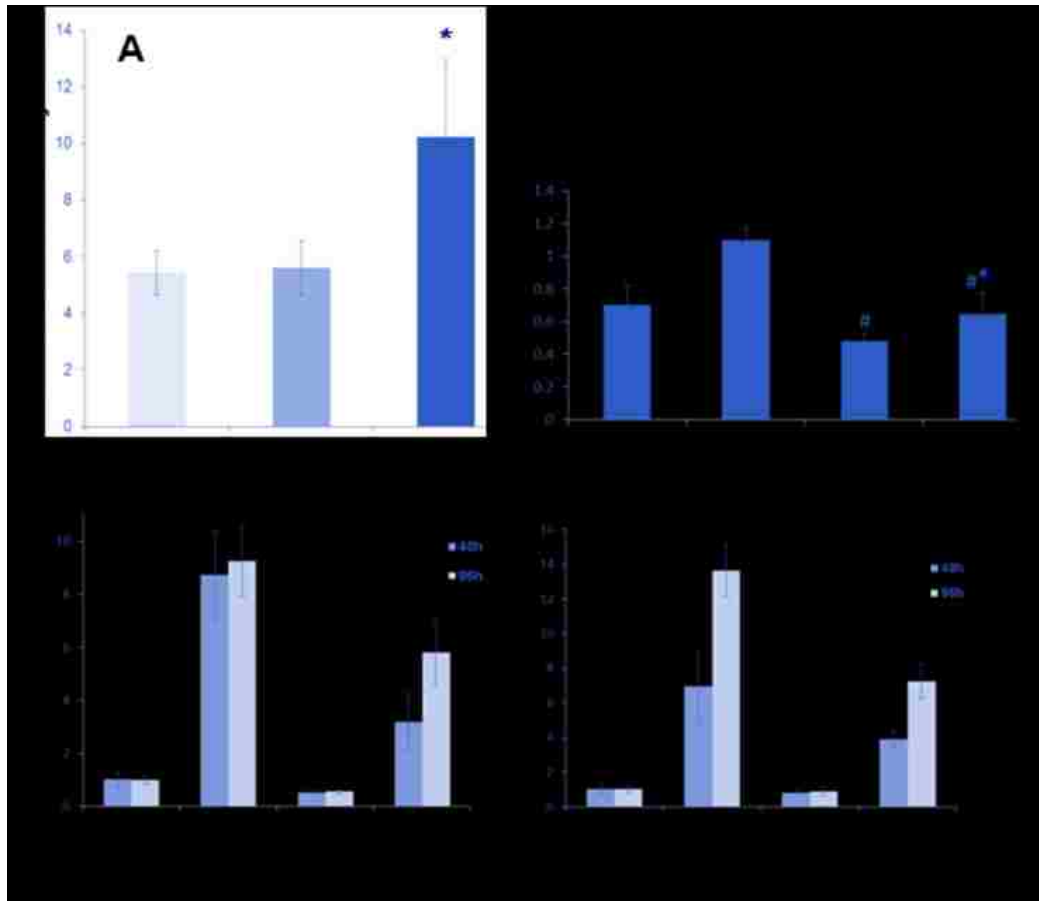


Figure 3. A. Activation of an XRE/DRE luciferase reporter was observed with TQ, but not VE. B. siRNA against AHR was used to knockdown AHR protein expression (NC = scrambled negative control). C. & D. AHR RNAi experiments to determine the modulation of AHR. C. and CYP1A1. D. gene expression by TQ treatment at 48 and 96 h after treatment. Quantitative PCR was used to measure AHR and CYP1A1 mRNA levels.

To further confirm the activation of the AHR by TQ mouse embryonic fibroblasts (MEFs) were acquired from AHR knockout mice, mice hemizygous for the AHR, and wild-type mice. The heterozygous and knockout MEFs were treated with vitamin E (VE), TQ, and benzo(a)pyrene (BaP); and CYP1A1 induction was measured 4 d after treatment. The wild-type and knockout MEFs were treated with tert-butylquinone (tBQ), pentamethylchromanol (PMCol), and TQ for 4 d. CYP1A1 mRNA levels were measured

as a marker of AHR activation. The results from this experiment showed a significant increase on the levels of CYP1A1 mRNA which was found intriguing as the structure of tBQ and TQ do not resemble the typical dioxin like structure which is thought to be responsible for AHR activation.

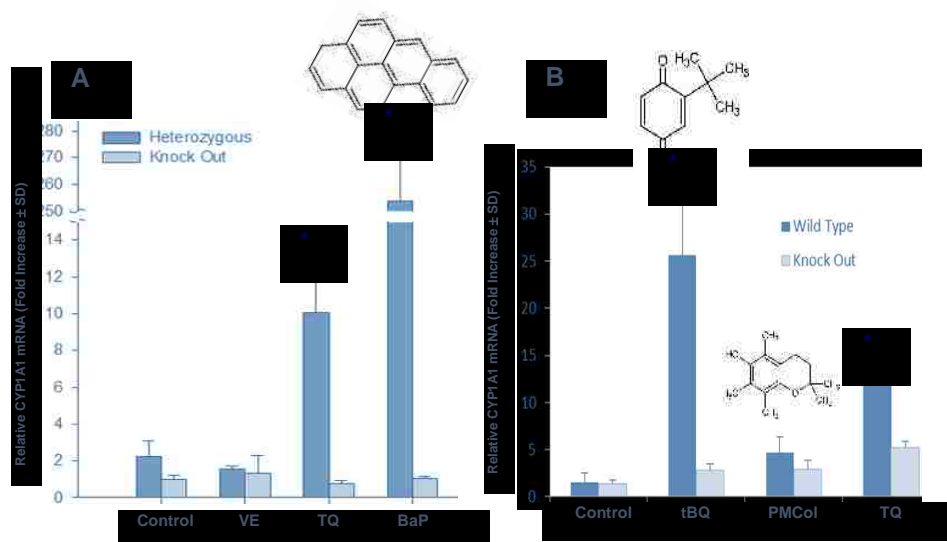


Figure 4. A. Heterozygous and knockout MEFs were treated with vitamin E (VE), TQ, and benzo(a)pyrene (BaP); and CYP1A1 induction was measured 4 d after treatment. B. Wild-type and knockout MEFs were treated with tert-butylquinone (tBQ), pentamethylchromanol (PMCoI), and TQ for 4 d. CYP1A1 mRNA levels were measured as a marker of AHR activation. (*P<0.05).

Rationale for Investigating Quinones

Quinones structures like tBQ, which were unanticipated chemical structures to be activators of the AHR, were identified as activators of the AHR, which in turn increases the scope of chemical structures recognized to activate the AHR. Although our results further support that the AHR is not highly selective, unique structure-activity relationships

were found that will assist identifying AHR pharmacophores. From the compounds investigated in addition to the Prestwick Chemical Library, tBQ was found to be an activator of the AHR while duroquinone showed no AHR activity.

Considering the results observed from this augmented Prestwick Library screen and the previous studies performed in the Thompson laboratory, it was decided to further evaluate quinone structures by validating their interaction with the AHR and their potency to activate it. The main question addressed was if the number of substituted carbons available in the quinone structure had a relationship with the potency of the quinone structure to activate the AHR. From the findings during the Prestwick Library screening we propose that increasing the number of substitutions will in turn decrease the molecule's potency to activate the AHR. The molecules deemed appropriate to address this question was duroquinone, 2,3-dimethoxy-6-methyl- 1,4 benzoquinone, 2,5 dimethyl benzoquinone, 2,6-dimethylquinone, tertbutyl-benzoquinone, methylbenzoquinone, benzoquinone and 1,4 cyclohexandione (Figure 5).

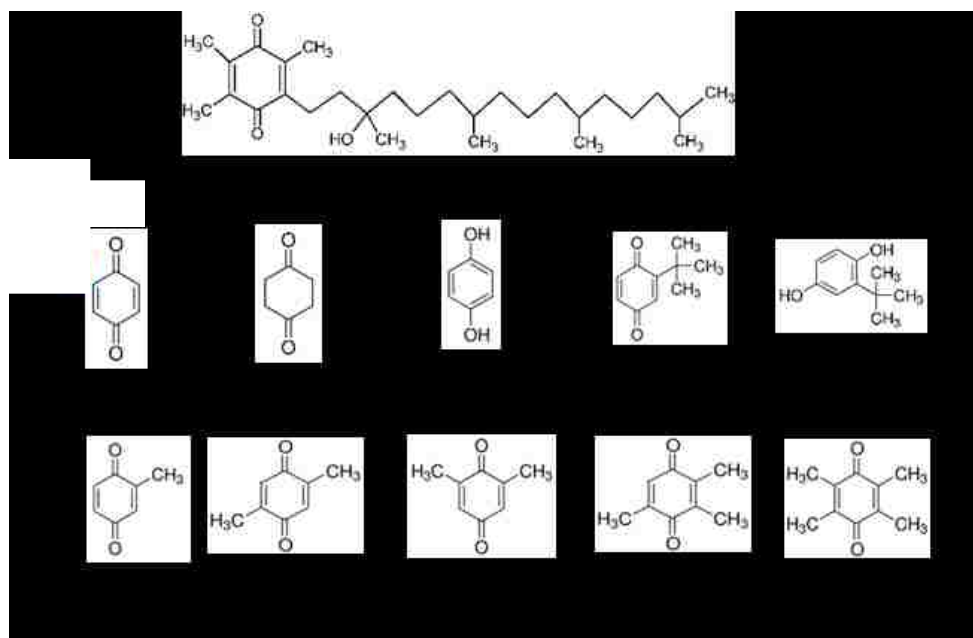


Figure 5. Quinone and related compounds analyzed for AHR activation using the AHRA assay based on the lead compound, tocoferylquinone (TQ).

Thesis Objectives:

1. Characterize the chemical functional groups necessary for less toxic compounds to act as AHR ligands.
2. Evaluate which attributes of functional groups determine the potency for activating the AHR.
3. Increase the number of known ligands of the AHR.

References

1. Benson JM, Shepherd DM. Aryl hydrocarbon receptor activation by TCDD reduces inflammation associated with Crohn's disease. *Toxicol Sci.* 120:68-78, 2011.
2. Bolton, JL, Dunlap T. Formation and biological targets of quinones: cytotoxic versus cytoprotective effects. *Chemical Research in Toxicology* 30: 13-37; 2017.
3. Delescluse C, Lemaire G, Sousa GD, Rahmani R. Is CYP1A1 induction always related to AHR signaling pathway? *Toxicology* 153:73-82, 2000.
4. Ehrlich AK, Kerkvliet NI. Is chronic AhR activation by rapidly metabolized ligands safe for the treatment of immune-mediated diseases? *Current Opinion in Toxicology* 2:72-78, 2017.
5. Hu W, Sorrentino C, Denison MS, Kolaja K, Fielden MR. Induction of Cyp1A1 is a nonspecific biomarker of aryl hydrocarbon receptor activation: results of large scale screening of pharmaceuticals and toxicants in vivo and in vitro. *Molecular Pharmacology* 71:1475–1486, 2007.
6. Jönsson ME1, Franks DG, Woodin BR, Jenny MJ, Garrick RA, Behrendt L, Hahn ME, Stegeman JJ. The tryptophan photoproduct 6-formylindolo[3,2-b]carbazole (FICZ) binds multiple AHRs and induces multiple CYP1 genes via AHR2 in zebrafish. *Chemico-Biological Interactions* 181: 447-454, 2009.
7. Jie Jack Li and E.J. Corey (eds.) *Drug Discovery: Practices, Processes, and Perspectives*. John Wiley and Sons, Hoboken New Jersey, 2013.
8. Oprea TI, Nielsen SK, Ursu O, Yang JJ, Taboureau O, Mathias SL, Kouskoumvekaki L, Sklar LA, Bologna CG.. Associating Drugs, Targets and Clinical Outcomes into an

- Integrated Network Affords a New Platform for Computer-Aided Drug Repurposing. *Molecular Informatics* 30: 100-111, 2011.
9. Pesatori AC1, Consonni D, Bachetti S, Zocchetti C, Bonzini M, Baccarelli A, Bertazzi PA. Short- and long-term morbidity and mortality in the population exposed to dioxin after the "Seveso accident". *Ind Health*. 41:127-138, 2003.
 10. Puga A, Ma C, Marlowe JL. The aryl hydrocarbon receptor cross-talks with multiple signal transduction pathways. *Biochemical Pharmacology* 77: 713-722 2009.
 11. Murray IA, Perdew GH. Ligand activation of the Ah receptor contributes to gastrointestinal homeostasis. *Current Opinion in Toxicology* 2: 15-23, 2017.
 12. Stockinger B, Di Meglio P, Gialitakis M, Duarte JH. The aryl hydrocarbon receptor: multitasking in the immune system. *Annual Reviews of Immunology* 32: 403-432, 2014.
 13. Vondráček J, Machala M, Bryja V, Chramostová K, Krcmár P, Dietrich C, Hampl A, Kozubík A. Aryl hydrocarbon receptor-activating polychlorinated biphenyls and their hydroxylated metabolites induce cell proliferation in contact-inhibited rat liver epithelial cells. *Toxicological Sciences* 83: 53-63, 2005.
 14. Wang Q, Yang K, Han B, Sheng B, Yin J, Pu A, Li L, Sun L, Yu M, Qiu Y, Xiao W, Yang H. Aryl hydrocarbon receptor inhibits inflammation in DSS-induced colitis via the MK2/p-MK2/TTP pathway. *International Journal of Molecular Medicine* 41: 868-876, 2017.

**CHAPTER 2: DIFFERENTIAL ARYL HYDROCARBON
RECEPTOR ACTIVATION BY SUBSTITUTED QUINONES**

Abstract

The aryl hydrocarbon receptor (AHR) is a polyfunctional, ligand activated transcription factor that serves as a sensor for environmental toxicants. Physiological actions of the AHR, such as activity in inflammation, support ongoing efforts to identify pharmacological modulators of the AHR (Ehrlich and Kerkvliet, 2017). In an effort to identify drug-like modulators of the AHR, an AHR reporter assay was developed. The pMMTVdsEGFP vector was modified to be AHR responsive via the incorporation of a dioxin response element into the MMTV promoter. Caco2 or HepG2 cells expressing a green fluorescence protein (GFP) based reporter sensitive were used to assess AHR activation. Cells stimulated by AHR activation express GFP, which can readily be quantified as the number of GFP positive cells, was found to be dependent on the potency of the ligand used to activate the AHR. This novel method is referred to as the Aryl Hydrocarbon Receptor Activation (AHRA) assay. The AHRA assay was originally validated using a FICZ dose-response with a Z factor of 0.28 achieved in Caco2 cells and 0.52 in HepG2 cells. In addition to screening the Prestwick Chemical Library, a library of 1,280 small molecules, most of which are agency approved, a collection of quinone containing compounds was also screened. From these screens, 8 off-patent drugs were identified from the Prestwick Chemical Library. In addition, the oxidation product of vitamin E, tocopherylquinone (TQ), was found to activate the AHR. TQ has a quinone functional group, which was chosen as a lead functional group for detailed investigation. AHRA assay analysis of para-quinones containing different numbers of methyl substitutions were screened. Para-quinone itself was found to be a relatively potent activator of the AHR. A single methyl or butyl substitution to one of the carbons present

in the para-quinone structure increased the efficiency of AHR activation. However, additional substitutions decreased potency of AHR activation. Increased toxicity with two or three additional substitutions. However, the fully methyl substituted quinone, duroquinone, did not activate the AHR, even at high concentrations and had reduced toxicity compared to other quinones with zero to three substitutions. This finding is enigmatic in that the quinone structure of TQ is fully substituted. Independent of this unexpected finding, it was observed that quinone structures containing a single substitution may serve as useful functional groups in the design of novel AHR activators with therapeutic potential.

Introduction

The aryl hydrocarbon receptor (AHR) was first identified as a mediator of TCDD toxicity, a contaminant of the herbicide Agent Orange (Sorg O et al., 2014). Since then, many different natural and synthetic environmental toxicants have been identified as ligands for activating the AHR. AHR activation by these agents results in the induction of genes associated with xenobiotic metabolism (Vondracek et al., 2004). Thus, the AHR has for many years been considered to have a key role in serving as a sensor of exposure to environmental toxicants. More recently, potent AHR ligands of endogenous origin have been identified. Also, modulation of AHR activity has been shown as useful in the treatment of models of inflammation, such as chemically induced colitis (Ehrlich and Kerkvliet, 2017; Benson and Shepherd, 2011). However, ligands used for this purpose have established toxicities or are not otherwise recognized as safe for human use. A key purpose of this study is to identify drugs that activate the AHR with established value for use in humans.

The AHR is a ligand-activated basic helix-loop-helix transcription factor (Stockinger et al., 2014). Once activated, the AHR sheds chaperone proteins that help stabilize it in the uninduced state in the cytoplasm and it then translocates to the nucleus where heterodimerization occurs with its binding partner the Aryl Hydrocarbon Receptor Nuclear Translocator (ARNT) protein (Stockinger et al., 2014). ARNT is also a binding partner for HIF-1alpha where it was independently designated HIF-1beta. Though activation of the AHR is primarily associated with xenobiotic metabolizing enzymes, AHR activation has also been associated with actions in differentiation, adaptive and innate immune responses, and organ homeostasis (Roman et al., 2017). Thus, the AHR may serve as a pleiotropic mediator of cellular responses. Recently, additional protein-protein interactions have been identified for the AHR, which may enable unique cell-dependent responses of the AHR.

Recently, encouraging breakthroughs in utilizing old drugs for new uses have been reported (Sachs et al., 2017). This so called “drug repurposing” has allowed transitioning the use of a drug originally designated for use against a specific disease state to find additional utility in treatment of an entirely distinct disease state, where its action was not historically recognized as relevant. In fact, small molecule chemical libraries of such drugs have facilitated this effort, where high-throughput analysis of specific molecular or cellular responses can be facilitated. One such example is the Prestwick Chemical Library, which contains 1,280 small molecules of mostly off-patent drugs. In this study, a novel method that allows for high-throughput analysis of AHR activation was developed to allow screening the Prestwick Chemical Library in addition to other potential useful agents for repurposing.

The development of high-throughput methods for drug screening has greatly facilitated efforts in drug repurposing. Assays developed should provide an accurate assessment of key pathways associated with a pathological conditions meaningful for drug repurposing. Optimally, the assay would be sufficiently sensitive and robust to allow for screening of agents with high specificity of drug action. Cell based assays often have many favorable screening characteristics. For example, a favorable feature for cell-based assays is that they allow the screening of agents that alter ligand binding to transcription factors for alterations in transcriptional activation mediated by the ligand. This property is favorable compared to ligand binding assays, which, although they provide information on the ligand affinity for the receptor, they do not enable an understanding of how ligand binding modulates the transcriptional activity of the receptor. However, cell based assays typically do not allow for identifying a single action without the potential for off-target effects. For many cell based assays, it is critical to integrate additional assays for specificity of action and validation of on-target effects. In this study, a flexible cell-based assay was developed to screen for drugs that activate the AHR and was designated, the “Aryl Hydrocarbon Receptor Activation” (AHRA) assay.

Materials and Methods

Chemicals

The Prestwick Chemical Library, a chemical library of 1,280 small molecules, mostly off-patent, approved drugs (e.g., FDA), was obtained from Prestwick Chemical (Illkirch, France). Vitamin E as dl- α -tocopherol and most other chemicals were obtained from Millipore Sigma (St. Louis, MO), unless specified otherwise. 2,3,5-trimethyl-1,4-

benzoquinone was obtained from Manchester Organics (Runcorn, Cheshire, UK). dl- α -tocopherylquinone was obtained from Research Organics (Cleveland, OH).

Expression Vectors

To construct pTBXMG, the mouse Cyp1A1 DRE region as used to construct pMpap1.1 (El-Fouly et al., 1994) was cloned by PCR and subcloned into pMMTVdsEGFP (Thompson et al., 1993). To determine specificity of DRE driven responses using pTBXMG, the pMMTVdsEGFP vector was used in place of pTBXMG. The pCSCMVdtTomato vector was used for transfection normalization as specified below.

Cell Culture and Transfection

Caco2 human colon adenocarcinoma cells and HepG2 human hepatocellular carcinoma cells (ATCC, Manassas, VA). Caco2 cells were maintained in Eagle's Minimal Essential Medium (EMEM) + 15% fetal bovine serum (FBS, Invitrogen, Carlsbad, CA), and 1% penicillin/ streptomycin. For Caco2 cells electroporation buffer was put in the hood and allowed to reach room temperature before use electroporation. Caco2 cells were transferred to a 15 ml sterile polypropylene tube and centrifuged for 5 minutes at 800-1000 rpm for 5 minutes. After centrifugation the cells were resuspended in 400 μ L of electroporation buffer and 20 μ g of the plasmid pTBXMG plasmid was added. The cells were then mixed and transferred to an electroporation cuvette to undergo electroporation. The optimal settings for electroporation were voltage 250V, mode 1V, and pulse 10ms, number of pulses 1, with unipolar polarity. After electroporation cells were resuspended in 12 mL of Caco2 media and transferred to a 96 well plate. Cells were incubated for 24 hours before Prestwick Library treatment. HepG2 cells were maintained

in Minimal Essential Medium (MEM) + 10% fetal bovine serum (FBS, Invitrogen, Carlsbad, CA), and 1% penicillin/streptomycin. For the Aryl Hydrocarbon Receptor Assay (AHRA), HepG2 cells were plated 24 h prior to transfection in 96-well flat-bottomed tissue culture plates at 12,500 cells per well. Cells were transfected with pTBXMG and pCSCMVtdTomato (Addgene) at a ratio of 1:100, respectively, using FuGENE 6 according to the manufacturers' instructions (Promega, Madison, WI). To test for non-specific MMTV promoter activation (i.e., not mediated by the AR), cells were transfected with pMMTVdsEGFP (Thompson et al., 1993) in place of pTBXMG using FuGENE 6, as described above. Treatments were administered 24 h after transfection. Chemicals from the Prestwick Chemical Library were screened at a final concentration of 10 μ M. All other AHRA chemical screening used concentrations, as specified.

EGFP Reporter Assay Validation

In order to evaluate pTBXMG as a reporter of AHR activation a dose response with 6-Formylindolo [3,2-b] carbazole (FICZ) was performed. FICZ is a well-established potent activator of the AHR. Thus, pTBXMG transfected cells treated with FICZ are expected to emit green fluorescent signal with an increasing signal as the dose of FICZ is increased. On the contrary, cells treated with FICZ vehicle control are not expected to emit green fluorescent signal. The dose-response was from 0 to 100 nM. Maximal FICZ response occurred at 10 nM (Fig.2). With toxicity observed at higher doses. Hence, we established that the optimal dose for FICZ as a positive control was 10nm which was used in the sub sequential analysis.

Cell Growth and Viability Analyses

Relative cell viability changes were determined using LNCaP and LAPC4 cells plated in 12-well tissue culture plates. Cell viability was determined by trypan blue dye (0.4%; Sigma, St. Louis, MO) exclusion determined by cell count using a hemacytometer and light microscopy. Cell growth analysis were performed using DU145, LNCaP, and LAPC4 cells plated in 96-well tissue culture plates. Relative cell numbers with and without TQ and VE treatment were determined using the CyQUANT NF Cell Proliferation Assay Kit (Invitrogen), according to kit instructions.

Microscopic Analyses and AHRA Quantification

Both light and fluorescent microscopy was performed using an Olympus IX70 Inverted Fluorescent Microscope equipped with an Olympus DP72 camera. Olympus cellSens Dimension 1.13 Life Science Imaging Software (Olympus, Waltham, MA) was used for image capture. To quantify the AHRA, the number of GFP positive cells (excitation at 488 nm) were visually quantified in a vertical scan through each well of a 96-well plate using a 10× objective and 10× eyepiece with an overall magnification of 100×.

Statistical Analyses

Significant differences in values between groups were assessed using an unpaired *t*-test with SigmaStat 3.1 software (Systat Software, Inc., San Jose, CA). *P* values less than 0.05 were used to signify statistical significance. Studies were performed as specified with a minimum of 3 samples (i.e., $n \geq 3$).

Results

Aryl Hydrocarbon Receptor Activation Assay

Studies were performed to evaluate the ability of small molecules to activate the AHR. Initially, a small molecule screening assay was developed by producing a green fluorescence reporter vector driven by an AHR responsive promoter (Figure 1).



Figure 1. Development of the Aryl Hydrocarbon Receptor Activation (AHRA) assay for high throughput screening of AHR activation. A. Construction of an AHR responsive reporter vector pTBXMG was used to screen for AHR activation used for Aryl Hydrocarbon Receptor Activation (AHRA) assay development. B. Sequence of actions for performing the AHRA assay. C. Photomicrograph of GFP positive cells (blue arrow) showing cells with significant AHR activation. Red arrow shows a tdTomato positive cell used for normalization of transfection (100 \times).

The next series of studies were performed to validate the activity of the AHRA assay.

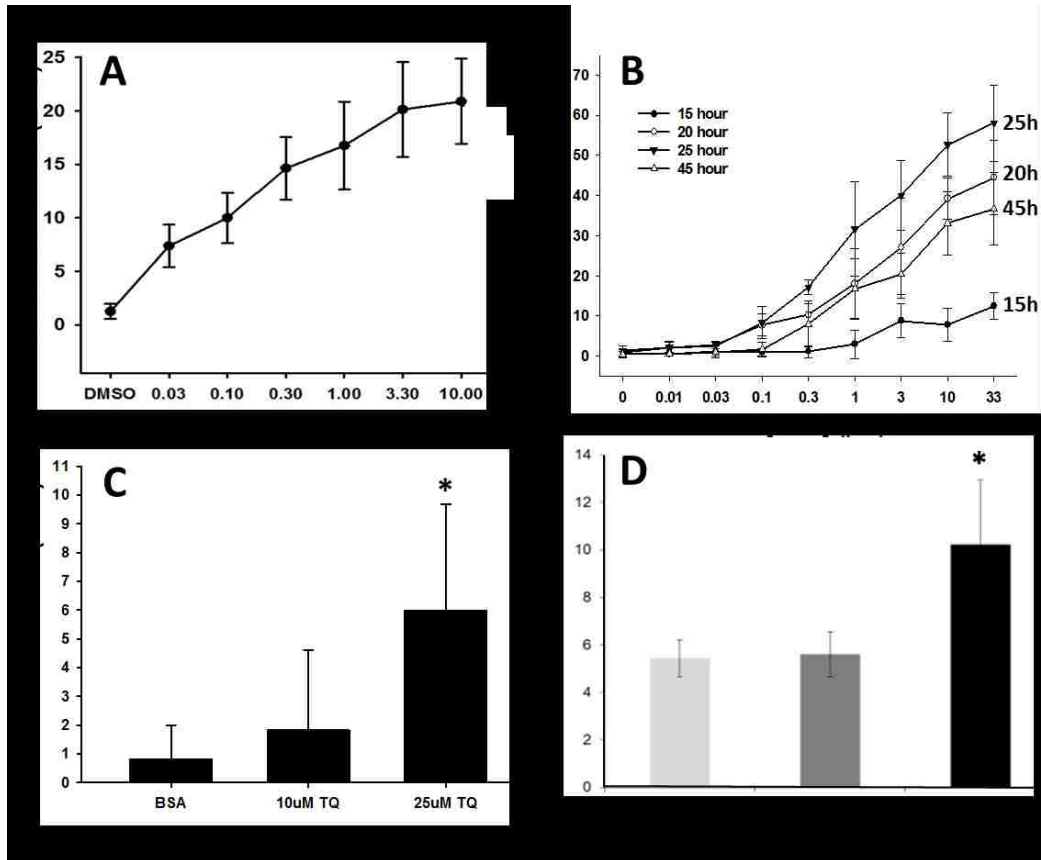


Figure 2. Assays used to examine AHR activation. A. FICZ dose-response curve using the AHRA assay in Caco2 cells. B. Kinetic analysis of AHRA assay efficiency at 15, 20, 25, and 45 h after treatment with a dose-response to FICZ in Caco2 cells. C. AHRA assay for analysis of TQ AHR activation in Caco2 cells (* $P < 0.05$). D. Validation of TQ AHR response using the pGudLuc6.1 vector for analysis of AHR activation in LNCaP human prostate cancer cells. Luciferase is the reporter for this assay (* $P < 0.05$).

Prestwick Library Analysis

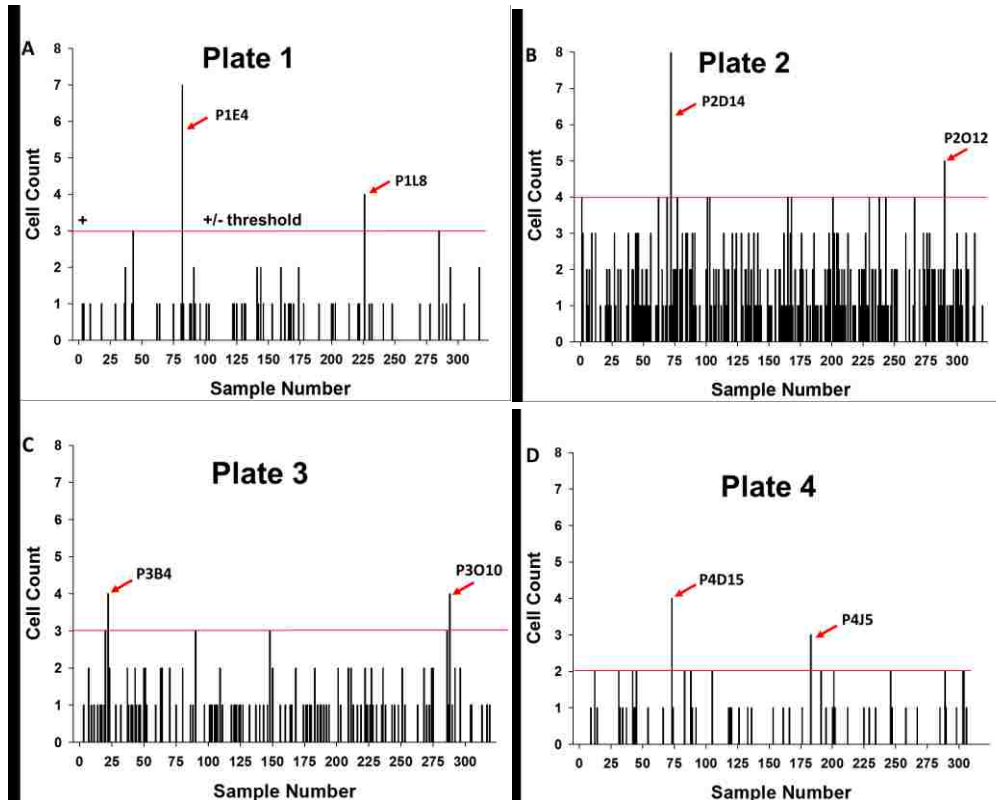


Figure 3. Results from the Prestwick Chemical Library Screen using the AHRA assay in Caco2 cells. Each plate represents the analysis of 320 compounds for a total of 1,280 compounds analyzed. Threshold cut off is based on the FICZ positive control (not shown due to scale distortion) and background levels of activity. A. For Plate 1, the threshold was set at 3; P1E4 and P1L8 gave above threshold values. B. For Plate 2, P2D14 and P2O12 gave above threshold values. C. For Plate 3, the threshold was set at 3; P3B4 and P3O10 gave values above threshold. D. For Plate 4, the threshold as set at 2; P4D15 and P4J5 values were above this threshold.

Multiple categories of chemically related structural groups were identified. Comparison to known AHR ligands revealed many structures with potential ligand activity. From these structures, we performed dose responses of the structures we thought

had a relationship with well-known AHR ligands. The first drug we compared with a well-known AHR ligand was P1E4 (Figure 4) the doses we chose for this compound dose response were 0.003, 0.01, .03, .1, .3, 1, 3, 10, and 33 μM . P1E4 was shown to have a significant AHR activation at 0.1 μM and increased its response all the way until 33 μM with no significance cell toxicity shown. (Figure 5)



Figure 4. A pharmacophore comparison of PAH a well established AHR activator and P1E4.

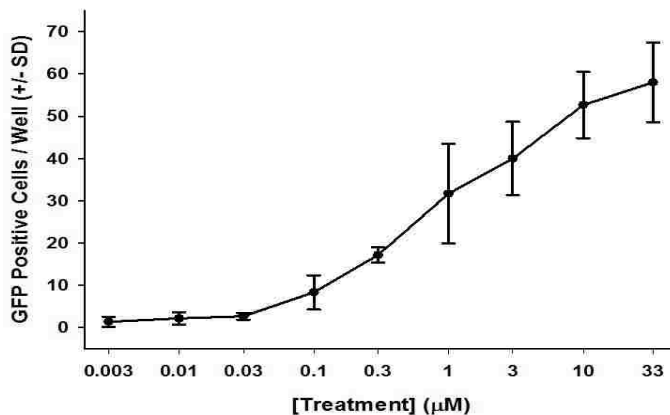


Figure 5. P1E4 dose response in Caco2 cells. The maximum effective dose found at 33 μM with no significance effect in toxicity.

Another drug we decided to pursue was the drug in the well P4D15 (Figure 6), this drug had similarities with the well-known AHR activator FICZ. For the drug

response of this drug we used the doses 0.01, .1, 1 and 10 μM where we started to see a significant response at 10 μM with no significance toxicity (Figure 7).

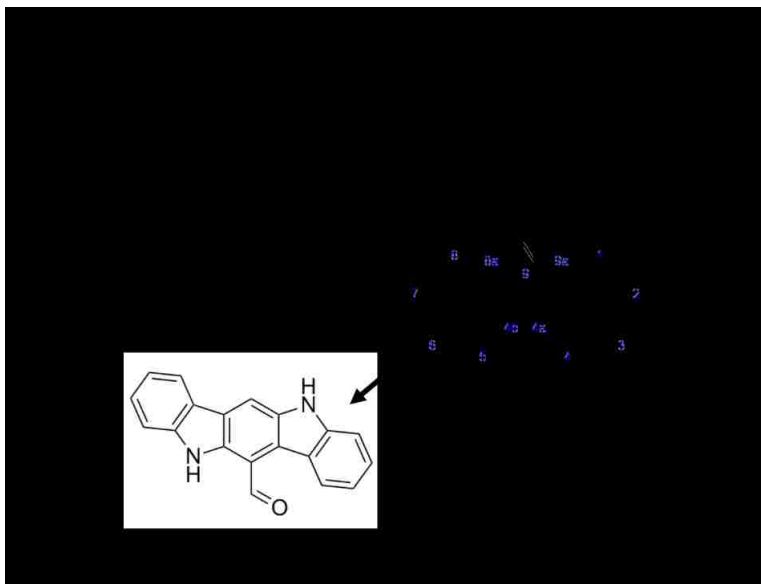


Figure. 6 is a pharmacophore comparison of FICZ a well established AHR activator and P1E4.

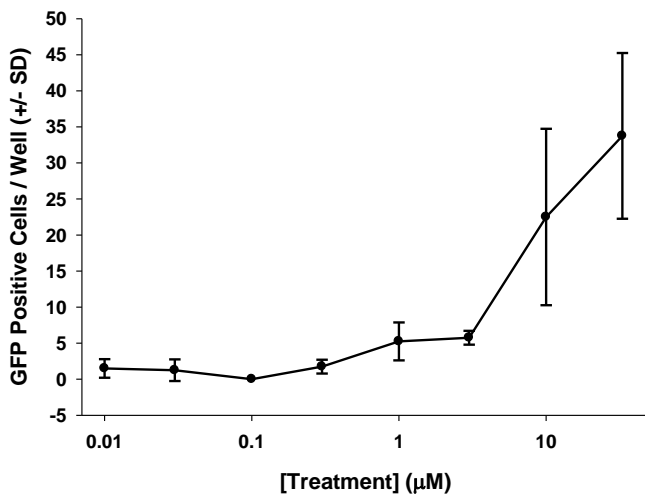


Figure 7. P4D15 dose response in Caco2 cells. The maximum effective dose was found at 33 μM with no significance effect in toxicity.

Cells were seeded in a 96 well plate at a density of 12.5×10^4 cells per well and allowed to incubate at 37°C for 24 hours before transfection. For the method for

transfection, HepG2 cells were transfected using FuGene6. The method for transfection and treatment was as follows: In a sterile polypropylene tube, 500 μL of serum-free medium were added followed by 15 μL of FuGENE 6. After the addition of FuGENE 6 the pTBXMG plasmid was added followed by the tomato plasmid. After the addition of both plasmids the tube was tapped gently to mix and was then incubated for at least 15 minutes. After incubation the medium-free serum with the plasmids was transferred to each well of the 96-well plate (5 μL per well). After successful delivery of the plasmid, the cells were incubated for 24 hours before treatment. The analysis was carried out 24 hours after the treatment of the quinone of interest.

Quinone Structure Analysis

For benzoquinone dose response the doses used were 3.75, 7.5, 15, 30, and 60 μM (Figure 8.). This structure was chosen as it provided a quinone structure with the least amount of substituted carbons in the para-quinone structure in order to test the hypothesis in question.

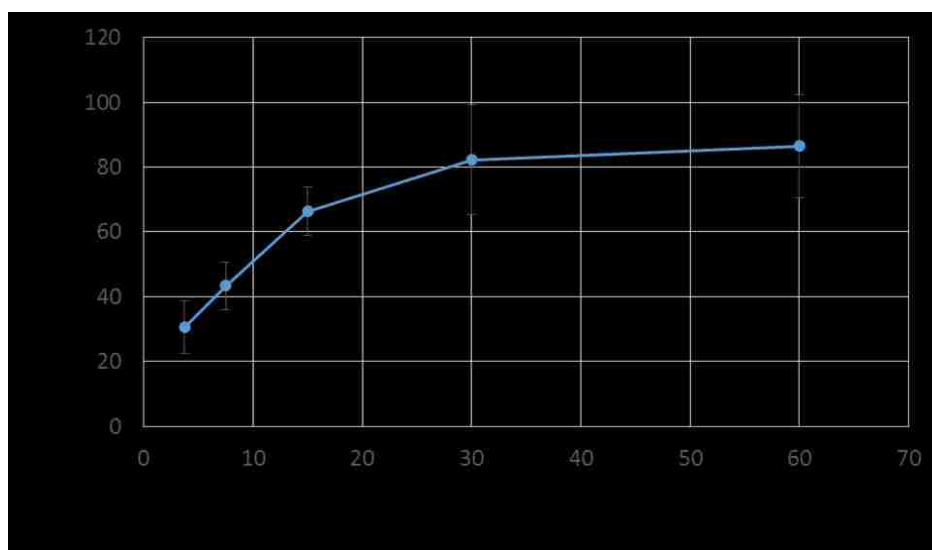


Figure 8. Benzoquinone showed to be an activator of the AHR with no significant toxicity.

In contrast with this we choose a quinone that lacked double bounds in its structure making it not a quinone but similar to the para-quinone structure. The chemical used was 1,4 cyclohexadione (Figure 9) with comparable doses to benzoquinone.

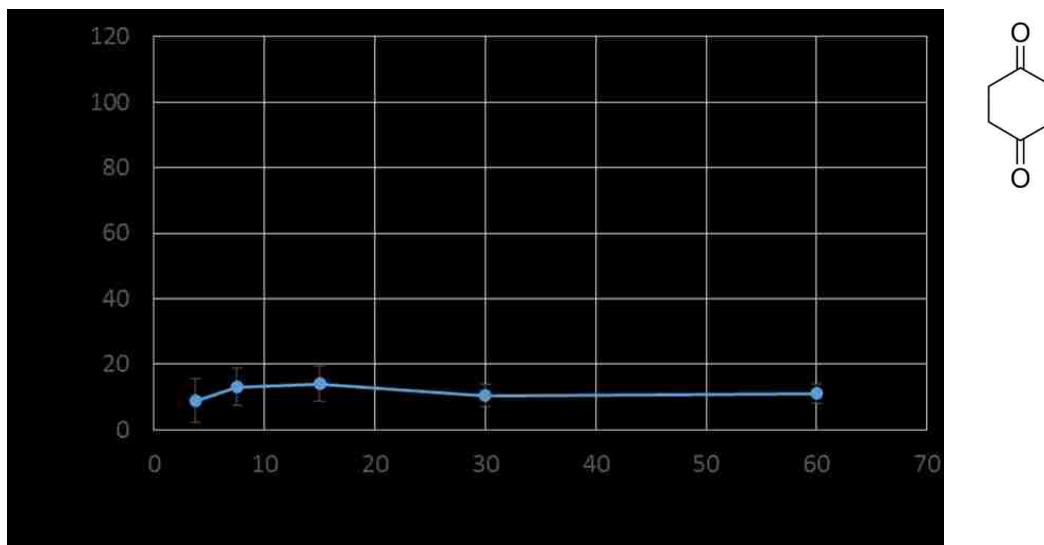


Figure 9. Even at high doses, 1,4 Cyclohexadione showed no AHR activity.

For the methylbenzoquinone dose response the doses used were 0.5, 1, 5, 10, 25, 50, 60, and 70μM (Figure 10).

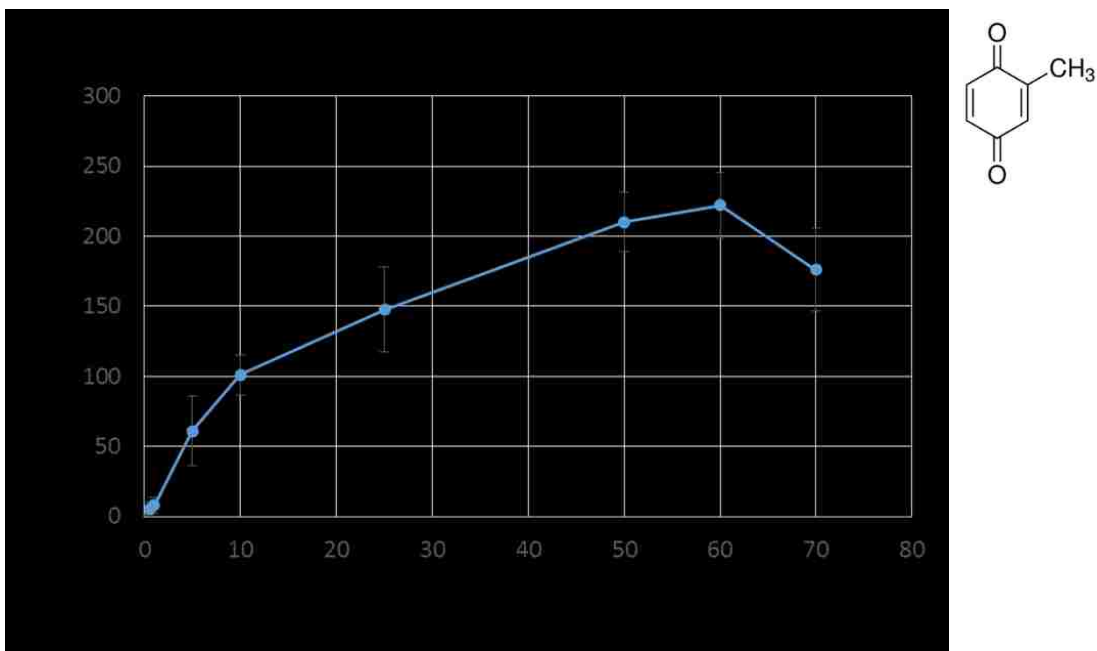


Figure 10. Methylbenzoquinone showed higher potency when compared with tBQ with the highest response at 60μM and showing a decrease to response probably due to toxicity at 70 μM.

For the tBQ dose response, the doses chosen were 0.03, 1, 3, 10, 33, 50 μL

(Figure 11).

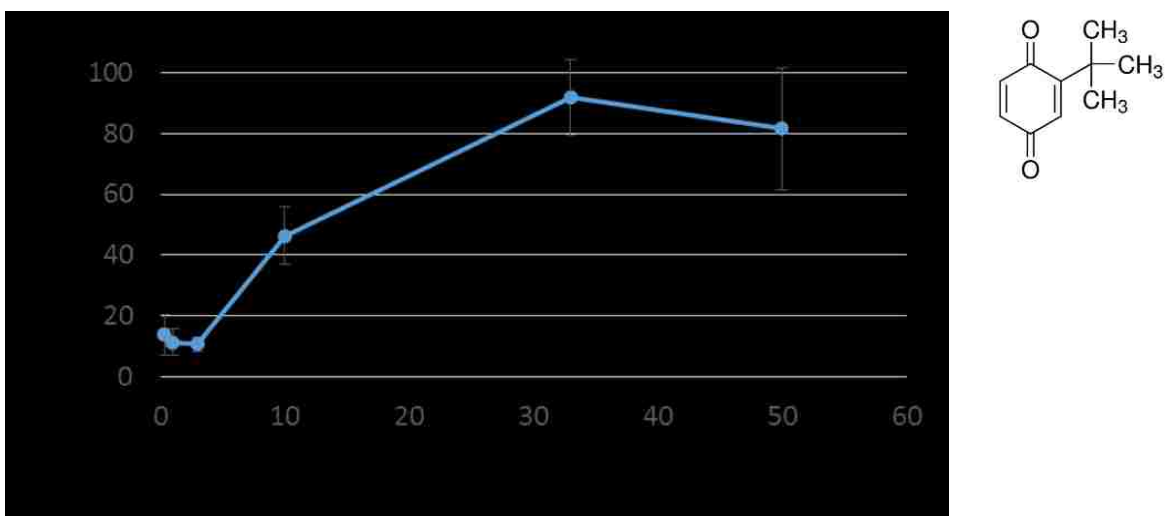


Figure 11. tBQ was agonist of the AHR, showing highest response at 33 μL, followed by cell toxicity at 50 μL.

As shown in the following graph for 2,6-dimethyl benzoquinone dose-response we used the same doses that we used for methylbenzoquinone (Figure 12).

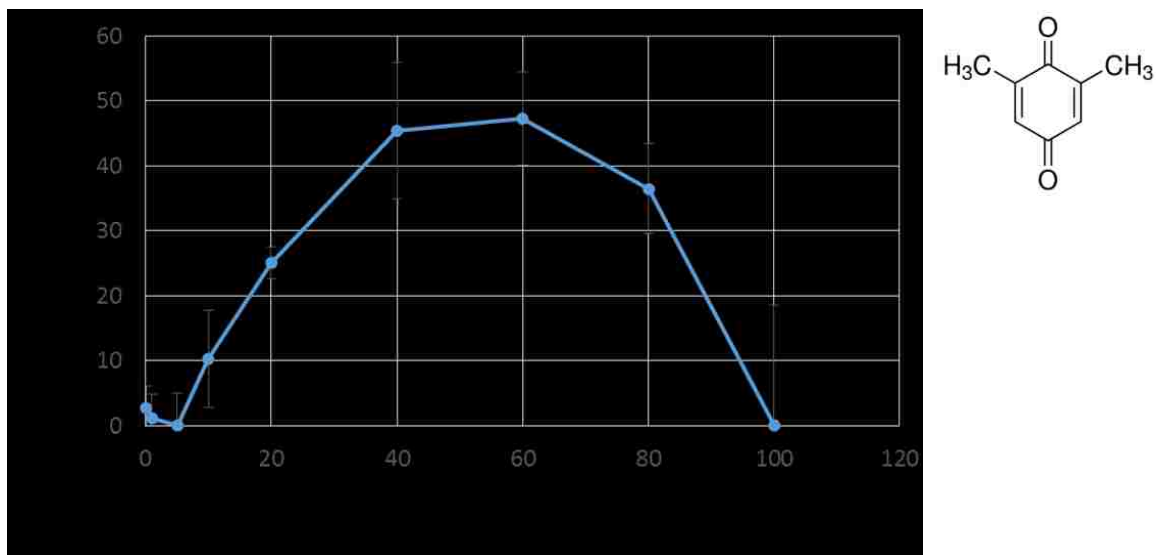


Figure 12. 2,6-dimethylbenzoquinone showed to be less potent when compared to tBQ and methylbenzoquinone. With the highest response at 60 μM and decrease in response probably due to cell toxicity at 80 μM.

For 2,5 Dimethyl benzoquinone dose response the same doses that were used for methylbenzoquinone were used (Figure 13).

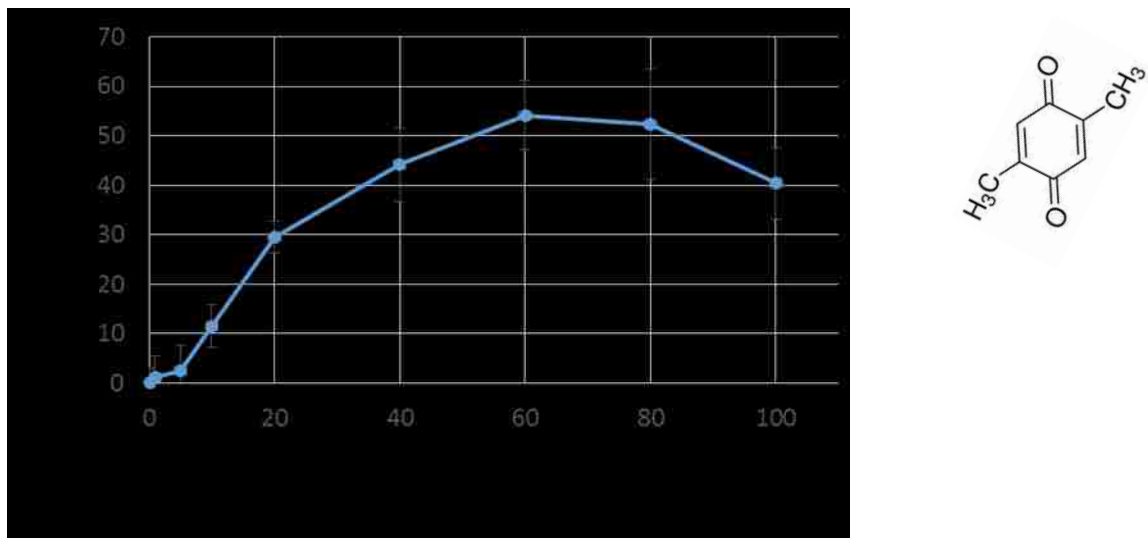


Figure 13. 2,5 dimethylbenzoquinone showed to be less potent when compared to tBQ and methylbenzoquinone as well but in contrast to 2,6 dimethyl benzoquinone, 2,5

dimethylbenzoquinone was more potent and less toxic. With the highest response at 60 uM and decrease in response probably due to cell toxicity at 80uM.

For the trimethylquinone (TMQ) a dose-response of 1, 3, 6, 12, 25 and 50µM more chosen (Figure 14). In contrast with the previous paraquinones, TMQ did not showed a significant activation when compared to control, nor it show a change between doses.

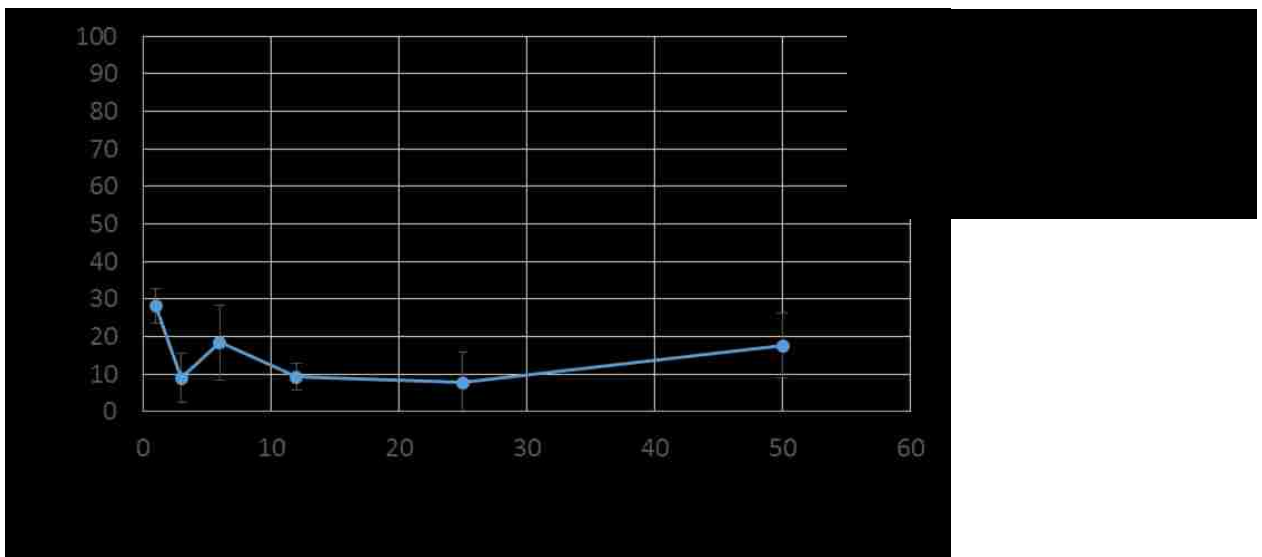


Figure 14. Trimethylquinone (TMQ) did not show a significant activation when compared to control, nor it show a change between doses.

For the duroquinone the same doses and dose increments as tBQ dose-response were chosen (Figure 15).

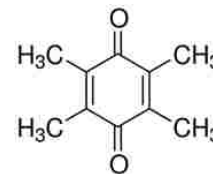
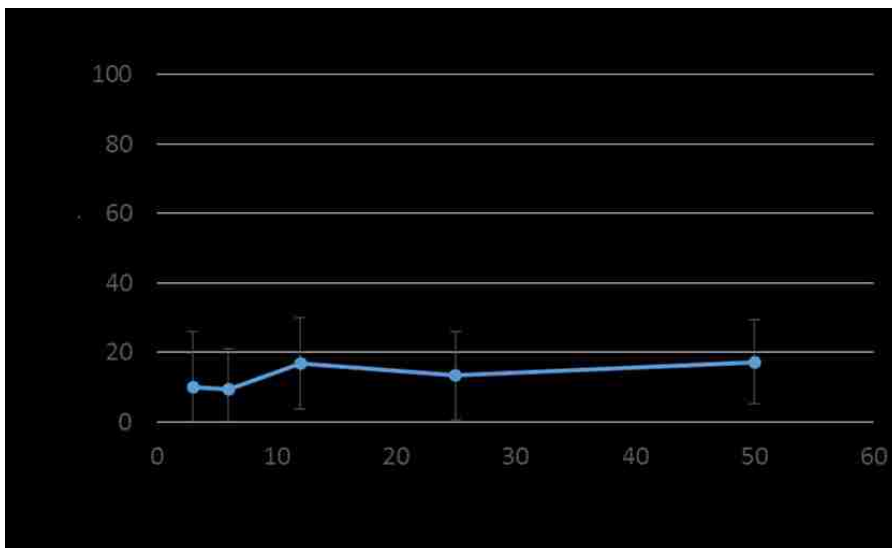


Figure 15. Duroquinone, similarly to TMQ showed no significance activation when compared to control. Nor it showed any change between doses.

Tert-butyl hydroquinone (TBHQ) (Figure 16), the reduced form of tBQ; and HQ (Figure 17), the reduced form of BQ were also analyzed.

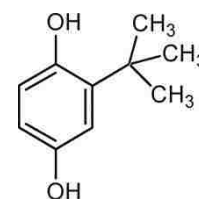
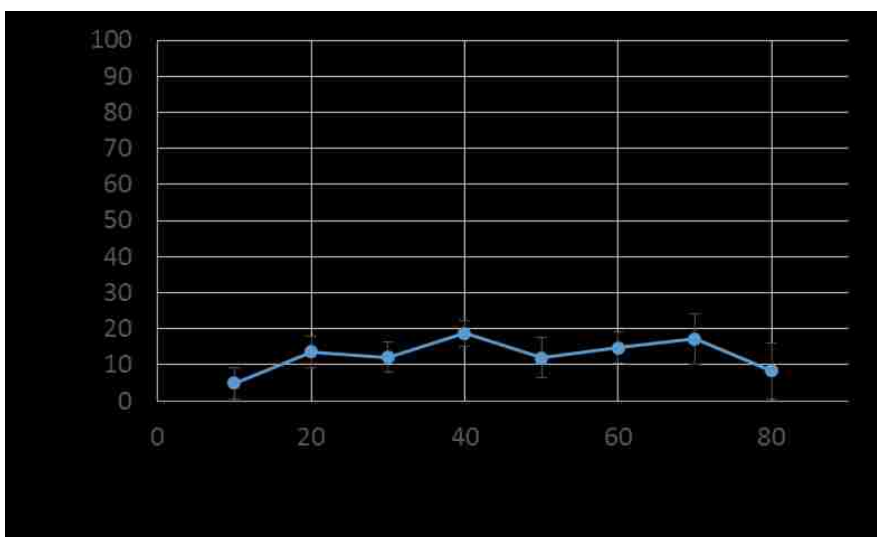


Figure 16. Reducing tBQ to TBHQ seemed to have abrogated the activity of the paraquinone to activate the AHR.

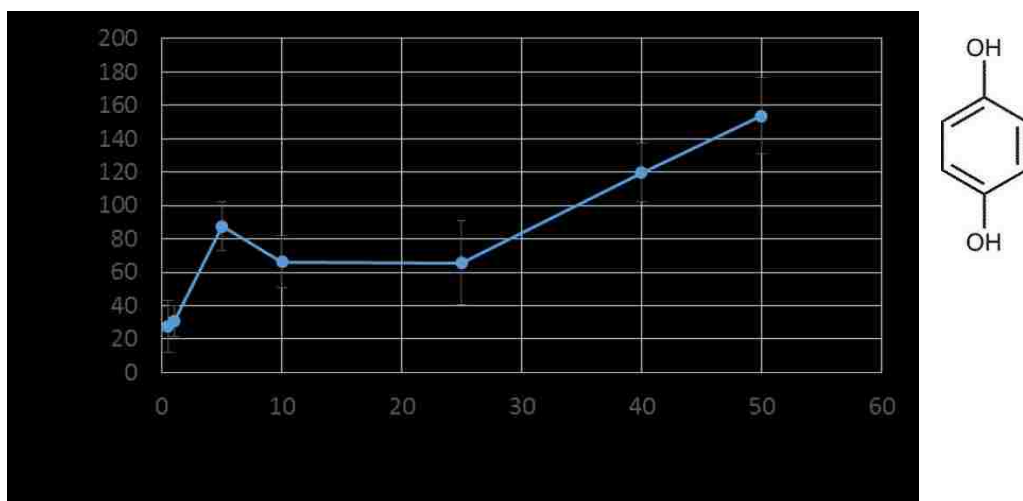


Figure 17. Contrary to the findings seen in the reduced form of tBQ, reducing BQ to HQ showed an increase in AHR activity.

After finding different para-quinones with AHR activity it was necessary to further validate that the emission of green fluorescent light was dependent to AHR activation and not activation of the MMTV portion by itself nor activation by the glucocorticoid response element. Therefore an experiment was carried out transfecting the cells only with MMTV, lacking the dioxin response element portion. In the experiment, the cells were treated with the different ligands we found at 25 μ M (Figure 18). Additionally we used dexamethasone as our positive control as the MMTV plasmid would be activated if there was binding in the glucocorticoid response element. Dexamethasone, a glucocorticoid, is an established activator of MMTV promoter activity in cells expressing a glucocorticoid receptor. In this study, dexamethasone was found to effectively stimulate the MMTV promoter in pMMTVdsEGFP (Figure 18). However, none of the quinone structures investigated were found to activate the MMTV promoter that did not contain a DRE suggesting that quinone activation of GFP expression from pTBXMG was dependent on the presence of a DRE (Figure 18).

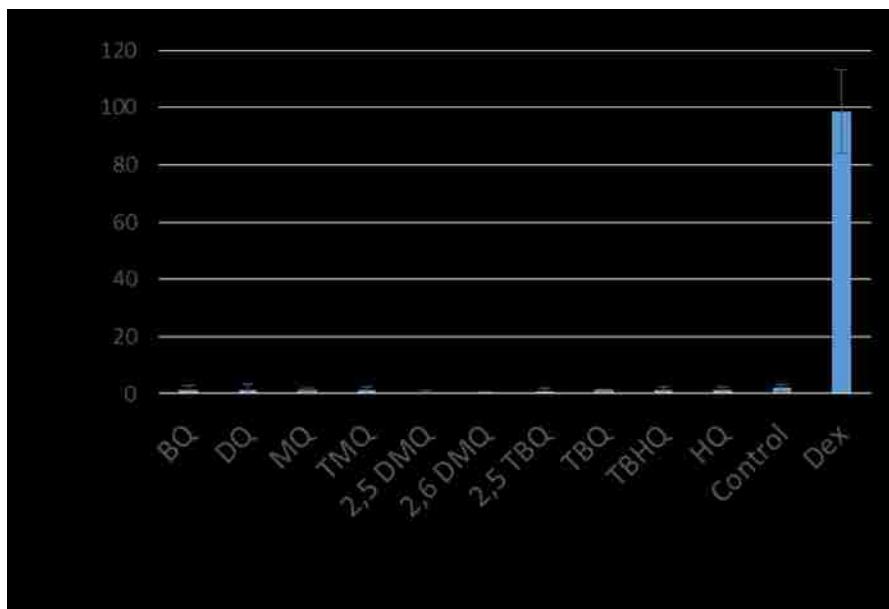


Figure 18. Treatment of cells transfected with plasmid lacking the dioxin response element with para-quinones did not emit green fluorescent light compared to the cells treated with dexamethasone.

Cytotoxicity was determined for each quinone using the CyQuant assay. Select quinone analysis of toxicity produced by DQ, BQ, MQ, and 2, 6 dimethylquinone is shown in Figure 19.

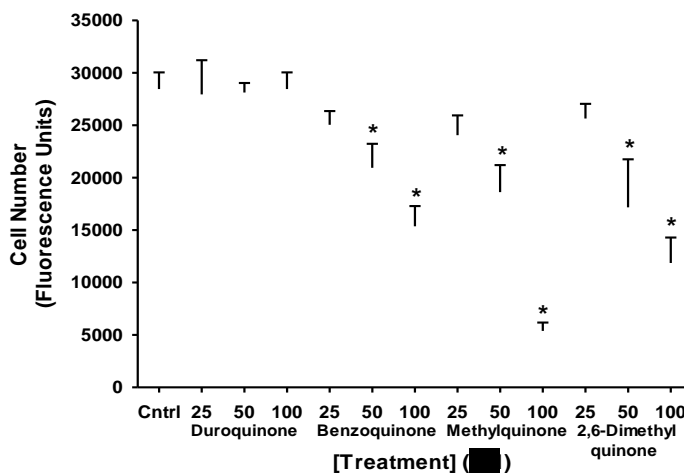


Figure 19. Quinone toxicity assessed 24 h after treatment for duroquinone, benzoquinone, methylquinone, and 2,6 dimethyl quinone at 25, 50, and 100 μM.

AHRA assay activation for each quinone at 25 μM was also assessed illustrating significant differences in the potency of each quinone (Figure 20).

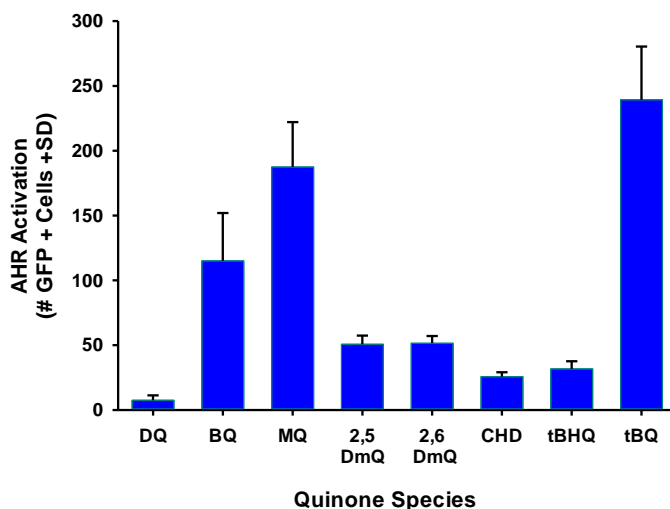


Figure 20. Quinone activation of the AHR was assessed using the AHRA assay 24 h after treatment.

Table 1 shows collective quinone data for EC_{50} , AHRA assay results at 25 μM , as well as 24 h viability data at 25 and 50 μM for HepG2 cells.

Table 1. Potency and toxicity data for the para-quinones investigated in HepG2 cells

Quinone	EC_{50} (μM)	AHRA Assay at 25 μM	Viability 25 μM (% control)	Viability 50 μM (% control)
Benzoquinone (BQ)	7.5	115	88	74
1,4 Cyclohexanedione (CHD)	NA ¹	26	93	104
tert-Butylquinone (tBQ)	10	239	88	77
tert-Butylhydroquinone (tBHQ)	NA ¹	32	111	99
Methylbenzoquinone (MQ)	10	187.5	85	66
2,5-Dimethylbenzoquinone (2,5DmQ)	18	51	92	89
2,6-Dimethylbenzoquinone (2,6DmQ)	20	52	90	61
2,3,5-Trimethylbenzoquinone (2,3,5TmQ)	NA ¹	10	95	85
Duroquinone (DQ)	NA ¹	7.5	98	99
Tocopherylquinone (TQ)	ND ²	ND ²	103	101

¹ No AHR activity up to the highest concentration investigated.

² Not determined.

Discussion

In this study, a highly flexible cell-based high-throughput assay for screening drugs that modulate AHR activity was successfully developed and designated the AHRA assay. There was a difference observed in the assay sensitivity between Caco2 cells and HEPG2 cells that could be accounted to different levels of AHR expression between the cell lines or due to the different transfection methods. Further studies would be necessary in order to elucidate which factor made the difference in sensitivity between the assay.

From the Prestwick Chemical Library, 8 distinct compounds were recognized as relatively potent AHR activators, which have not previously been recognized as altering AHR activity. In addition, the oxidation product of vitamin E, tocopherylquinone (TQ), was found to activate the AHR. As TQ has been investigated as a treatment for diseases such as Friedrich's Ataxia (Lynch et al., 2012), TQ was pursued as a "lead compound" for further drug repurposing. The quinone component of TQ was found to be an essential functional group for TQ's ability to activate the AHR. Therefore, quinones similar to the structure found in TQ were investigated as chemical structural variants to identify those with the greatest potential for activating the AHR. Interestingly, substitution of both the type and number of groups on the para-quinone structure was found to have a significant impact on the ability of quinones to activate the AHR. The information acquired in this research should prove useful in novel drug design for safe and effective agents to modulate AHR activity therapeutically.

The dose response analysis of different quinone structures with different number of carbon substitutions showed a direct relationship with the number of positive cells after treatment. When comparing the potencies of the quinone structures to activate the AHR

there is a significant decrease as the number of substituted carbons reaches 2 and higher. Another thing that is important to note is that the structure of the quinone is not the only thing necessary to activate the AHR as the experiment comparing benzoquinone with 1,4 cyclohexanedione showed that the ability of the structure without double bonds completely lost its potency to activate the AHR regardless of structure. From these studies we believe that some of these quinones such as TQ have the potential to be used as a novel treatment of inflammatory bowel disease as this structure showed a significant potency to activate the AHR without causing significant toxicity to the HepG2 Cells.

References

1. Benson JM, Shepherd DM. Aryl hydrocarbon receptor activation by TCDD reduces inflammation associated with Crohn's disease. *Toxicol Sci.* 120:68-78, 2011.
2. Bolton, JL, Dunlap T. Formation and biological targets of quinones: cytotoxic versus cytoprotective effects. *Chemical Research in Toxicology* 30: 13-37, 2017.
3. Delescluse C, Lemaire G, Sousa GD, Rahmani R. Is CYP1A1 induction always related to AHR signaling pathway? *Toxicology* 153:73-82, 2000.
4. Ehrlich AK, Kerkvliet NI. Is chronic AhR activation by rapidly metabolized ligands safe for the treatment of immune-mediated diseases? *Current Opinion in Toxicology* 2:72-78, 2017.
5. El-Fouly MH, Richter C, Giesy JP, Denison MS. Production of a novel recombinant cell line for use as a bioassay system for detection of 2,3,7,8-tetrachlorodibenzo-p-dioxin-like chemicals. *Env Toxicol Chem* 13: 1581-1588, 1994.
6. Hu W, Sorrentino C, Denison MS, Kolaja K, Fielden MR. Induction of Cyp1A1 is a nonspecific biomarker of aryl hydrocarbon receptor activation: results of large scale screening of pharmaceuticals and toxicants in vivo and in vitro. *Molecular Pharmacology* 71:1475–1486, 2007.
7. Jönsson ME1, Franks DG, Woodin BR, Jenny MJ, Garrick RA, Behrendt L, Hahn ME, Stegeman JJ. The tryptophan photoproduct 6-formylindolo[3,2-b]carbazole (FICZ) binds multiple AHRs and induces multiple CYP1 genes via AHR2 in zebrafish. *Chemico-Biological Interactions* 181: 447-454, 2009.
8. Jie Jack Li and E.J. Corey (eds.) *Drug Discovery Practices, Processes, and Perspectives*. John Wiley and Sons, Hoboken New Jersey, 2013.

9. Lynch DR, Willi SM, Wilson RB, Cotticelli MG, Brigatti KW, Deutsch EC, Kucheruk O, Shrader W, Rioux P, Miller G, Hawi A, Sciascia T. A0001 in Friedreich ataxia: biochemical characterization and effects in a clinical trial. *Mov Disord* 27:1026-1033, 2012.
10. Oprea TI, Nielsen SK, Ursu O, Yang JJ, Taboureau O, Mathias SL, Kouskoumvekaki L, Sklar LA, Bologna CG.. Associating Drugs, Targets and Clinical Outcomes into an Integrated Network Affords a New Platform for Computer-Aided Drug Repurposing. *Molecular Informatics* 30: 100-111, 2011.
11. Puga A, Ma C, Marlowe JL. The aryl hydrocarbon receptor cross-talks with multiple signal transduction pathways. *Biochemical Pharmacology* 77: 713-722 2009.
12. Murray IA, Perdew GH. Ligand activation of the Ah receptor contributes to gastrointestinal homeostasis. *Current Opinion in Toxicology* 2: 15-23, 2017.
13. Sorg O AhR signalling and dioxin toxicity. *Toxicol Lett* 15:230:225-333, 2014.
14. Stockinger B, Di Meglio P, Gialitakis M, Duarte JH. The aryl hydrocarbon receptor: multitasking in the immune system. *Annual Reviews of Immunology* 32: 403-432, 2014.
15. Thompson TA, Gould MN, Burkholder JK, Yang NS. Transient promoter activity in primary rat mammary epithelial cells evaluated using particle bombardment gene transfer. *In Vitro Cellular and Developmental Biology* 29A: 165-170, 1993.
16. Vondráček J, Machala M, Bryja V, Chramostová K, Krcmár P, Dietrich C, Hampl A, Kozubík A. Aryl hydrocarbon receptor-activating polychlorinated biphenyls and their hydroxylated metabolites induce cell proliferation in contact-inhibited rat liver epithelial cells. *Toxicological Sciences* 83: 53-63, 2005.

17. Wang Q, Yang K, Han B, Sheng B, Yin J, Pu A, Li L, Sun L, Yu M, Qiu Y, Xiao W, Yang H. Aryl hydrocarbon receptor inhibits inflammation in DSS-induced colitis via the MK2/p-MK2/TTP pathway. *International Journal of Molecular Medicine* 41: 868-876, 2017.

CHAPTER 3: CONCLUSIONS AND FUTURE STUDIES

Conclusion

From the results provided by the dose responses of different quinone structures with variation on carbon substitution it can be concluded that quinone activation of the AHR is dependent on the number of substituted carbons in the para-quinone structure. As seen by our experiments, one of the structures with most activity for the AHR was BQ and as the number of substitutions on the structure increases by either methylation or reduction; so did their activity for activating the AHR. However, we also observed that adding a methyl group to the BQ increased its potency for AHR activation, eluding to the fact that AHR activation by para-quinone structures is not only dependent on the number of substitutions on the para-quinone structure, but the size and the characteristics of the groups on each carbon, as well.

Future Directions

The data presented on this thesis begins to address pharmacophore relationships of para-quinones and AHR activation. I have presented that para-quinones have the ability to activate the AHR given that they fulfil a certain number available unsubstituted carbons in their structure. In addition, I have shown that there is a relationship between the number substitutions in para-quinones and their toxicity. This section will focus on addressing additional questions that arose from these studies and validation studies necessary for further pharmacologic considerations of the AHR.

Validation Studies

The hypothesis driving the study was; Established drugs serve as model compounds to evaluate the aryl hydrocarbon receptor as a pharmacologic target. To begin

addressing the hypothesis, quinones were identified as lead compounds, through an AHR-EGFP reporter assay. One of the first studies that should be performed in order to validate our assay is the use of HepG2 cells with AHR knockout transfected with the pTBXMG plasmid. If the number of positive cells becomes nonexistent it would provide further evidence that our assay is dependent on AHR activation. Another thing to consider is that the pathway of AHR activation is complex and activation of the AHR can be independent of para-quinone binding to the AHR. For example, CYP1A1 is responsible for metabolizing both xenobiotic and endogenous ligands of the AHR. Hence, inhibition of CYP1A1 may cause an accumulation of other natural compounds in the cells which may result in an indirect activation of the AHR. Thus, I propose two different studies to discard AHR activation through CYP1A1 blockade as the pathway responsible for AHR activation by para-quinones. The first study proposed is the measurement of ethoxyresorufin-O-deethylase (EROD) activity. CYP1A1 mediates the deethylation of 7-ethoxyresorufin (7-ER) to form resorufin (Whyte and Jung 2008). Consequently, the concentration of resorufin produced per mg/protein/minute is indicative of CYP1A1 activity (Kennedy and Jones 1994). If the para-quinones activate the AHR through CYP1A1 blockage, it would be expected for the EROD assay to report a low concentration of resorufin in addition of reported AHR activation. The second study that can shed light to this question is evaluating whether or not para-quinones are substrates of CYP1A1 and the rate by which CYP1A1 is able to metabolize para-quinones into inactive-compounds. As mentioned before, CYP1A1 is responsible for metabolizing activators of the AHR. As a result, the activation of the AHR could be skewed due to a low rate of metabolism and an increase time of exposure of the AHR to the para-quinone. An additional study to validate AHR activation is the

measurement of CYP1A1 up regulation through a western blot analysis. Both of these studies in addition to our EGFP reporter assay would help provide stronger evidence of AHR activation by our lead compounds.

In addition to the CYP1A1 validation studies it would be important to have a better understanding of the relationship of para-quinone AHR activation and CYP1A1. The proposed mechanism to investigate this question in a greater detail is the use of cells with CYP1A1 knockout. There are multiple outcomes that could occur with this experiment including but not limited to; an increase in AHR activation or no change in the amount of AHR activation. From all these different possible outcomes critical information could be drawn to further understand the involvement of CYP1A1 and para-quinone AHR activation. For instance, an increase in the activation of AHR in CYP1A1 knockout cells could mean that the para-quinone is a ligand for CYP1A1 and that CYP1A1 may be necessary for the metabolism of the ligand, which may be an interesting finding as it could also change the toxicity seen by the para-quinone. On the other hand, no change in AHR activation may support the idea that AHR activation by para-quinones is independent of CYP1A1.

Future Studies

In this thesis I have shown novel ligands with the ability to activate the AHR but the question about their use in pharmacotherapy is still elusive. This section will be focused on my suggestions of the studies that would need to be done before using this compounds in pharmacotherapy.

Understanding Aryl Hydrocarbon Receptor's Role in Biology

It has already been established that the AHR plays a role in immunology, including inflammation (Stockinger et al., 2014). But there is still a discrepancy on the actual function of the AHR and the contribution that it has in immunology which I believe is attributed to the fact that the AHR has multiple ligands. Therefore, the outcome of activating the AHR has to be an independent consideration for each ligand. Due to this concept I propose that cell studies be performed with our proposed ligands TQ, BQ, and MQ to figure out which ligand results in the modulation of inflammatory responses through AHR activation. Screening for proteins and cytokines involved in inflammation is a possibility to assess the ligands involvement in inflammation. Among the different cytokines and proteins, interleukin-22 (IL-22) stands out as a possible biomarker for AHR mediated inflammation. Kiyomatsu-Oda recently published a study that looked at the potential of FICZ to treat chronic eczema. In the study Kiyomatsu-Oda stimulated HaCaT cells and normal human epidermal keratinocytes (NHEKs) with or without FICZ and then performed quantitative reverse transcriptase polymerase chain reaction, immunofluorescence, and siRNA treatment. In the study Kiyomatsu-Oda utilized atopic dermatitis-like NC/Nga murine model and treated the mice for 2 weeks with either Vaseline as a control, FICZ ointment, or betamethasone 17-valerate ointment (Kiyomatsu-Oda et al., 2018) The results from the study showed that FICZ reduced atopic dermatitis-like skin inflammation and expression of IL-22 through AHR activation in mice (Kiyomatsu-Oda et al., 2018)

In addition to the immunology cell studies there also needs to be animal experiments that look deeper into the AHR function. For these experiments, genetically

engineering mice with double knock out of the AHR in different parts of the body could be very useful. It would be important to know the difference in tissue and embryonic development these mice undergo after removing the expression of the AHR. The reason why it would be important to perform the experiments in different tissue is to further understand if AHR function is dependent on its location.

Inflammatory Bowel Disease Applications

Currently the capabilities of TQ to reduce inflammation in mice after TNBS induced colitis is being tested with promising results. These unpublished results support the concept of using TQ as a possible alternative therapy for the treatment of inflammatory bowel disease. Nonetheless, toxicity studies have to be performed in mice in order to be able to determine what the minimum effective dose (MED) is and the minimum toxic dose in order to extrapolate the therapeutic index for TQ. Extrapolating the therapeutic index of TQ will help give a starting dose for starting experimental studies in humans. After efficacy and safety are established in humans a number of studies would need to be performed in order to establish if TQ has a place in therapy. These, studies would have to be non-inferiority studies comparing TQ with the current standard of care for inflammatory bowel disease.

Other Applications

Current treatments for immune mediated diseases have different limitations which I believe could be overcome by the use of the AHR as a pharmacological target. Among the complications of treating immune mediated diseases is the fact that many of these therapies are not specific and have systemic and long-lasting effects. For instance,

steroids which are a commonly used for the treatment of immune mediated diseases have effects such as tissue atrophy or adrenal suppression which can be seen even after stopping the drug. These side effects can be very significant and can limit the use of steroids to certain populations. Currently, monoclonal antibodies are a class of drugs that are more selective which can circumvent many of the problems that are faced by steroids. However, these therapies are still extremely expensive which makes it difficult to be used in therapy. Hence, AHR ligands present an opportunity to broaden our pool of agents used to treat immune mediated diseases as the proposed repurposed drugs in this studies are very cheap in comparison to the monoclonal antibodies and there is extensive data in each molecule. In this thesis it is proposed that there are many ligands that are already in the market that show low toxicity that could be repurposed for their use in immune mediated diseases. Also, according to the studies reviewed, the effects of the AHR are not long lasting after ligand exposure in contrast with steroids. The experiments that I suggest is the use of TQ as an adjunct therapy to the standard of care. Studies should be performed where there is a patient group with an immune mediated disease under standard of care plus placebo and comparing it to another group of patients taking TQ.

References

1. Kennedy SW, Jones SP. Simultaneous Measurement of Cytochrome P4501A Catalytic Activity and Total Protein Concentration with a Fluorescence Plate Reader. *Analytical Biochemistry* 222:217-223, 1994.
2. Kiyomatsu-Oda M, Uchi H2, Morino-Koga S3, Furue M4. Protective role of 6-formylindolo[3,2-b]carbazole (FICZ), an endogenous ligand for arylhydrocarbon receptor, in chronic mite-induced dermatitis. *Journal of Dermatological Science* pii: S0923-1811:30108-7, 2018.
3. Stockinger B, Di Meglio P, Gialitakis M, Duarte JH. The aryl hydrocarbon receptor: multitasking in the immune system. *Annual Reviews of Immunology* 32: 403-432, 2014.
4. Whyte JJ, Jung RE, Schmitt CJ, Tillitt DE. Ethoxyresorufin-O-deethylase (EROD) Activity in Fish as a Biomarker of Chemical Exposure. *Critical Reviews in Toxicology* 30:347-570, 2000.

APPENDICES

Appendix 1: Modulation of autophagic flux and cell death by the antihistamine astemizole in human prostate cancer cells

Teofilo Borunda^a, Debra A. MacKenzie^a, Chien-An Andy Hu^b, Harmony Bowles^a,
Kirsten A.M. White^c, Tamara L. Anderson Daniels^a, , Jeffrey P. Norenberg^a, Graham
Timmins^a, Todd A. Thompson^{a,*}

Authors affiliations:

^a Department of Pharmaceutical Sciences, The University of New Mexico College of Pharmacy, Albuquerque, NM 87131, United States

^b Department of Biochemistry and Molecular Biology, The University of New Mexico School of Medicine, Albuquerque, NM 87131, United States

^c Division of Epidemiology, Department of Medicine, University of New Mexico, Albuquerque, New Mexico

* Corresponding author at:

Department of Pharmaceutical Sciences
University of New Mexico College of Pharmacy
MSC09 5360

1 University of New Mexico
Albuquerque, New Mexico 87131

Tel.: 505-925-4710

E-mail address: tthompson@salud.unm.edu (T. A. Thompson)

Keywords Autophagy · Prostate Cancer · Astemizole

Abstract

The pharmacological modulation of autophagic processes is under investigation for treating a diverse group of human diseases including for cancer chemotherapy.

Autophagy is a homeostatic cellular pathway involved in the turnover of organelles, aggregated proteins, cell remodeling, and regeneration of nutrients, such as amino acids, for cell survival during stress. We have identified astemizole (AST) as an agent that inhibits growth, induces cell death, and modulates autophagy in prostate cancer cell lines. AST was found to visibly increase intracellular granularity in a dose-dependent manner in all human prostate cancer cell lines tested, including the androgen-sensitive 22Rv1 and LNCaP lines as well as in androgen-independent PC3 cells. Increased levels of intracellular granularity were quantified by side-scatter using flow cytometry.

Additionally, AST produced a dose-dependent decrease in cell growth and viability in all prostate cancer cell lines tested, where 22Rv1 cells were most sensitive and LNCaP cells were found to be most resistant. Higher doses of AST led to an abrupt cell death in prostate cancer cell lines. AST also increased punctae formation of EGFP-LC3 II and acridine orange staining of intracellular granules, strongly supporting alterations in autophagic pathways by AST. Docetaxel or radiation, an established modulator of autophagy, enhanced AST-induced cell killing. Cellular fragmentation was enhanced by the combination of radiation and AST. AST significantly increased LC3 II levels, showing AST to be a dose-dependent modulator of autophagic flux in prostate cancer cells. The combination of radiation and AST acted synergistically to increase LC3 II levels as a further indicator of cellular autophagy modulation. Together, results from these studies suggest that chemical modulators of autophagy such as AST shift the

balance of autophagic processes toward prostate cancer cell death that may prove to be a useful strategy for cancer treatment.

Introduction

Prostate cancer is the most frequently diagnosed form of cancer among men in the United States and a leading cause of cancer deaths (Jemal et al. 2017). Strategies for prostate cancer treatment are limited and, at present, rely principally on targeting androgenic activity, which promotes prostate cancer progression in early, advanced disease (Helsen et al. 2014). Despite an initial efficacy for this approach, prostate cancer invariably advances to a state refractory to antiandrogenic therapy. Targeting prostate cancer through mechanisms other than androgenic pathways relies on a thorough understanding of metabolic pathways essential to prostate cancer progression. Thus, targeting metabolic pathways important to prostate cancer progression may enable the development of novel therapies for this disease.

Autophagy, a cellular homeostatic system for recycling of metabolic substances, has been proposed as a target for cancer therapy. The process of autophagy can degrade aggregate proteins, protein complexes, and whole organelles (Van Limbergen et al. 2009). Under conditions of nutrient deprivation, this process may be activated to provide amino acids and fatty acids to sustain the basic energy needs of the cell (Kung et al. 2011). In this manner, the autophagic process allows both for efficient recycling of cellular components and for establishing a cellular metabolic balance between energy consumption and production (Levine and Klionsky 2004). Macroautophagy is an extensively investigated form of autophagy that is characterized by the formation and

accumulation of double membrane intermediate vesicles (Loos and Englebrect 2009). Macroautophagy is the process most commonly referenced simply as autophagy, which is the term used here.

To date, considerations to target autophagy for cancer therapy have proven controversial. This is in part due to an incomplete understanding of the dichotomy of autophagy's role in cell survival and cell death (Wu et al. 2012; Zhou et al. 2012). Gewirtz (2014) suggests that autophagic processes in cancer therapy have up to four functions. These include a cell protective function that, when inhibited, sensitizes cancer to therapies and a cytotoxic function that promotes cancer cell killing. Other proposed autophagic functions either do not affect cancer therapies or have a role in cytostasis where inhibition may produce resistance to cancer therapies (Gewirtz, 2014). Studies have shown that either insufficient or excessive levels of autophagy can signal cell death pathways, whereas intermediate levels can facilitate cell survival (Kang et al 2007). In prostate cancer therapy, preclinical data provides evidence that autophagy may be involved in therapeutic resistance and disease progression; yet inhibition of autophagy can enhance cell killing produced by cancer therapies (Farrow et al. 2014). The development of novel methods to modulate autophagy therapeutically would help resolve the ambiguity of autophagy in cancer therapy.

The Prestwick Chemical Library was screened using a high-throughput HyperCyt flow cytometry system to identify inducers of autophagy in prostate cancer cells (Haynes et al. 2009). The initial basis for the screening used side-scatter as an endpoint. The production of vacuolar structures, which may include autophagosome and autolysosome structures that lead to increased intracellular granularity. The agents present in the

Prestwick Chemical Library were selected for their high chemical and pharmacological diversity as well as for their known bioavailability and safety in humans and may prove useful for repurposing their therapeutic use (Oprea et al. 2011). The initial screening encompassed a diverse range of pharmacological activities, including the antihistamine, astemizole. In this study, astemizole was investigated for its potential to modulate autophagic and cell death pathways in prostate cancer cells.

Materials and Methods

Chemicals

Astemizole (AST), IGEPAL CA-630, pentamethylsulfonfyl fluoride, sodium dodecyl sulfate, aprotinin, sodium deoxycholate, and sodium orthovanadate were obtained from Sigma Aldrich (St. Louis, MO). Docetaxel was obtained from LC Laboratories (Woburn, MA).

Cell culture and cell culture reagents

The 22Rv1, LNCaP, and PC3 human prostate cancer cell lines were obtained from ATCC (Manassas, VA). Prostate cancer cell lines were maintained in Dulbecco's modified Eagle's medium (DMEM; Invitrogen, Carlsbad, CA) containing 5% heat-inactivated fetal calf serum (FCS; Sigma, St. Louis, MO) with streptomycin-penicillin antibiotics (designated F5A1) in a 5% CO₂ incubator at 37°C.

Cell viability and cell proliferation assays

Relative cell viability changes were determined using cells plated in 12-well tissue culture plates (Costar, Corning, NY) in F5A1 media at 3×10^4 cells per well. AST was administered at the specified concentrations with 1,000× stock solutions dissolved in

ethanol. Cell viability was determined using trypan blue dye (0.4%; Sigma, St. Louis, MO) exclusion and cell counts determined using a hemocytometer and light microscopy. Prostate cancer cell growth analyses were performed using LNCaP and PC3 cells plated in 96-well tissue culture plates (Costar, Corning, NY) initially plated at 1,000 cells per well in F5A1. Relative cell numbers with and without AST treatment were determined using the CyQUANT NF Cell Proliferation Assay Kit (Invitrogen), according to kit instructions.

Cellular granularity and fragmentation determinations using flow cytometry

For cellular granularity and fragmentation analysis, PC3 cells were plated in 12-well tissue culture plates (Costar, Corning, NY) at 3×10^4 cells per well. AST was administered at the specified concentrations using 1,000 \times stock solutions dissolved in ethanol. A BD FACScan System flow cytometer (BD Biosciences, San Jose, CA) was used for forward- and side-scatter measurements. FlowJo software (FLOWJO, LLC, Ashland, OR) was used for analysis of flow cytometric data. To determine levels of cellular fragmentation induced by radiation and AST, a BD Accuri™ C6 flow cytometer (BD Biosciences) was used with data analysis performed using Accuri™ C6 Software (BD Biosciences).

Radiation Exposures

For radiation exposures, PC3 or 22Rv1 cells were plated in 6-well tissue culture plates (Costar, Corning, NY) at 4×10^4 cells per well. AST was administered at the specified concentrations using 1,000 \times stock solutions dissolved in ethanol for the specified time periods. Cellular radiation exposures were performed using a Gammacell

40 (¹³⁷Cs) Irradiator (Atomic Energy of Canada, Ltd., Ottawa, ON, Canada), according to instrument instructions, available through the UNM Health Sciences Center at the radiation doses specified.

Immunoblotting

LC3 lipidation analysis as an increase in LC3 II was determined for AST. Cells were plated at a density of 10⁶ cells per 100 mm cell culture plate in 10 ml of DMEM/CSS and maintained in incubators at 37°C in 5% CO₂. After treatment with vehicle or AST, cells were washed in cold 1× PBS and lysed in a buffer containing 1.0 % IGEPAL CA-630, 0.5 % sodium deoxycholate, 0.1 % sodium dodecyl sulfate, 0.1 mg/ml phenylmethylsulfonyl fluoride, 1 mM sodium orthovanadate, and 10 µg/ml aprotinin in 1× PBS. Cell extracts were stored at -80°C until analysis. Sample protein levels were determined using the BCA Protein Assay kit (Pierce Biotechnology, Rockford, IL) according to kit instructions. Total protein (25 to 30 µg) from cell extracts were electrophoresed on 10-20% Criterion Precast gels (BioRad, Hercules, CA) and transferred to Immobilon-P membranes (Millipore Corp., Bedford, MA) using a GENIE wet transfer system (Idea Scientific, Minneapolis, MN). Membranes were blocked in Tris-buffered saline containing 5% nonfat dry milk at 4°C and incubated with anti-LC3 polyclonal antibody (PM036; MBL International, Woburn, MA) or mouse anti-β-actin antibody (A5441; Sigma). After washing, membranes were incubated with a secondary horseradish peroxidase-conjugated goat anti-rabbit (SouthernBiotech, Birmingham, AL) or anti-mouse IgG (Biomeda, Foster City, CA) and analyzed using Western Lightning Chemiluminescence Reagent Plus (PerkinElmer, Waltham, MA) on a ProteinSimple FluorChem R instrument (ProteinSimple, San Jose, CA) according to instrument

instructions. Band intensities were determined using Protein Simple Molecular Imaging Software.

PC3.EGFP-LC3 cell and acridine orange staining analysis

PC3.EGFP-LC3 cells, PC3 stably transfected with pEGFP-LC3, were generated as previously described using PC3 cells instead of LNCaP cells (Kaini, et al. 2012). PC3.EGFP-LC3 cells were treated with 10 μ M AST for 24 hours and then examined by fluorescent microscopy. To analyze acidic vesicles associated with autophagy, PC3 cells were treated for 24 hours with 10 μ M AST, wash with 1 \times PBS and then stained with the lysosomotropic agent acridine orange (ThermoFisher Scientific, Eugene, OR). Photomicrographs were obtained as specified under “*Light and fluorescent microscopy*”. Both PC3.EGFP-LC3 cell and acridine orange stained PC3 cells were analyzed using an excitation filter at 490.

Light and fluorescent microscopy

Both light and fluorescent photomicrographs were captured using an Olympus IX70 Inverted Fluorescent Microscope equipped with an Olympus DP72 camera. Olympus cellSens Dimension 1.13 Life Science Imaging Software (Olympus, Waltham, MA) was used for image capture.

Statistical Analysis

Significant differences in values between groups were assessed using an unpaired t-test with SigmaStat 3.1 software (Systat Software, Inc., San Jose, CA). P values less than 0.05 were used to signify statistical significance. Determination of tumor growth rate was performed using standard procedures for simple linear regression analyses. Determination of synergism between treatments were made as recommended for

GraphPad Prism (GraphPad Software, Inc., La Jolla, CA). Studies were performed as specified with a minimum of 3 samples per group (i.e., $n \geq 3$).

Results

The effects of AST on prostate cancer cell viability and proliferation in cell culture were determined. Trypan blue exclusion and hemocytometry was used to examine the dose-response of androgen-sensitive 22Rv1 and LNCaP cells and androgen-independent PC3 human prostate cancer cells after 48 h AST treatment (Fig. 1A). The androgen-sensitivity of the different prostate cancer cell lines did not determine sensitivity to AST-induced cell death as the androgen-sensitive 22Rv1 and LNCaP cells were found to be more sensitive and resistant to AST, respectively, than PC3 cells (Fig. 1A). The 22Rv1 cells were found to be most sensitive with significant cell death observed at 5 μM AST, whereas LNCaP and PC3 cells were not significantly affected at this dose of AST (Fig. 1A). PC3 cells were found to be affected by 10 μM AST and LNCaP cells were the most resistant to AST-induced cell death (Fig. 1A). Further analysis of AST effects on prostate cancer cell proliferation at non-lethal doses of AST (i.e., 0.5 to 5 μM AST) was determined over 96 h. PC3 cells showed a significant decrease in cell growth when treated with doses of 2.5 and 5 μM AST, but were unaffected by doses of 0.5 and 1.0 μM AST (Fig. 1B). LNCaP cells showed a decrease in cell proliferation at 5 μM AST, whereas the growth of these cells was not affected by doses of 0.5 to 2.5 μM AST (Fig. 1C). Significant cell death was observed in both PC3 and LNCaP cells treated with 10 μM AST for 96 h (Figs. 1B and 1C). Thus, the

sensitivity to AST on prostate cancer cell death and proliferation was dose and cell type specific.

We and others have reported the production of observable intracellular granularity in cells following treatment with a variety of drugs, including AST (Haynes et al. 2009; Jakhar et al. 2016). Fig. 2A, B, and C show the microscopic presentation of intracellular granularity in PC3 cells following treatment with 10 μ M AST compared to control, untreated cells. We have developed methods to quantify intracellular granularity by analyzing side-scatter (SSC) using flow cytometry (Haynes et al., 2009). For example, Fig. 2D and 2E shows the increase in SSC observed in PC3 cells following 48 h treatment with AST observed as SSC using flow cytometry. This method allows the quantification of increases in granularity induced by AST treatment. Fig. 2F shows the dose-response of AST-induced increases in SSC (i.e., granularity) after treatment of PC3 cells. PC3 cells showed 77% intracellular granularity after treatment with 3 μ M AST compared to 10% in untreated cells (Fig. 2F). Interestingly, cells with significant death, which was observed at 10 and 30 μ M AST, had lower levels of intracellular granularity compared to the peak levels observed with 3 μ M AST (Fig. 2F).

To determine if the induction of intracellular granularity was coincident with the induction of autophagy, biomarkers of autophagy were assessed after AST treatment in prostate cancer cells. An initial indication of autophagic induction in prostate cancer cells was provided by the observation of the production of punctae in PC3 prostate cancer cells stably expressing EGFP linked to the LC3 protein, a useful marker of autophagy (Fig. 3A – control, untreated; Fig. 3B – AST treated). An additional assay for autophagy was performed showing acridine orange staining of acidic autophagic vacuoles (Paglin et

al. 2001) in PC3 cells, producing a bright orange-red fluorescence (Fig. 3C – control, untreated; Fig. 3D – AST treated). An early event in autophagosome production is the lipidation of LC3 (i.e., ATG8; Klionsky et al. 2016). Formation of lipidated LC3 (LC3 II) is readily observed by immunoblotting. Fig. 3E demonstrates the induction of increased LC3 II expression following treatment of 22Rv1 prostate cancer cells with AST. Taken together, these studies provide strong evidence that AST can modulate autophagy in prostate cancer cells.

Radiation is used extensively in the treatment of prostate cancer (Pugh et al. 2013). Studies were performed to determine the effects of radiation combined with AST treatment on prostate cancer cell killing. Exposure to 5 and 10 Gy radiation resulted in decreased PC3 cell viability after 24 h (Fig. 4A). Doses of AST higher than 7 μ M significantly augmented radiation induced cell killing (Fig. 4A). The effects of combined radiation and AST were also examined for induction of autophagy. The combination of 5 Gy and 8 μ M AST, administered 1 h before radiation, synergistically increased levels of LC3 II protein after 24 h radiation exposure suggesting that the combination of radiation and AST significantly modulated autophagy in PC3 cells (Fig. 4B). Doses of AST and radiation that killed PC3 cells were found to significantly reduce cell numbers, below the cell numbers originally plated. To determine if these interventions induce PC3 cell bursting, cellular fragmentation was measured by scatter patterns using flow cytometry. Both 5 and 10 Gy radiation, 10 and 15 μ M AST, and the combination of each were found to increase cellular fragmentation (Fig. 4C, 4D, 4E, and 4F). Indeed, a close correlation between levels of cellular fragmentation and cell death induced by AST and radiation was observed. In addition to PC3 cells, the combination of radiation and AST was found

to enhance cell killing in 22Rv1 prostate cancer cells (Table 1). For example, the combination of 10 Gy radiation with 2, 4, or 8 μ M AST increased cell killing, where the combination of 10 Gy radiation and 4 or 8 μ M AST acted synergistically to enhance cell killing (Table 1). In addition, the combination of 10 nM docetaxel, used in the treatment of advanced, hormone-refractory prostate cancer, with 2, 4, or 8 μ M AST increased 22Rv1 cell killing (Table 1). Thus, radiation and chemotherapeutic prostate cancer cell killing was augmented by the co-administration of AST.

Discussion

The drug AST, a second-generation H1-receptor antagonist, has been considered for repurposing from its use as an antihistamine to other applications, including cancer chemotherapy (Garcia-Quiroz and Camacho, 2011). In this study, AST was shown to modulate autophagic and cell death pathways in human prostate cancer cells. Variability in the sensitivity to AST-induced cell death was observed among the prostate cancer cell lines examined, which included the androgen-sensitive 22Rv1 and LNCaP cells as well as the androgen-independent PC3 prostate cancer cell line. Due to the variation in AST response observed among androgen-sensitive prostate cancer cell lines, it is unlikely that the sensitivity of prostate cancer cell lines to AST-induced cell death is dependent on androgen responsiveness. Further, both increases in intracellular granularity and the modulation of autophagic pathways by AST were observed in all prostate cancer cell lines examined, independent of androgenic sensitivity of the cell line treated.

Although AST has not been investigated extensively as a potential therapeutic strategy in prostate cancer, it has demonstrated potential in other cancer cell types. For

example, de Guadalupe Chavez-Lopez et al. (2014) have shown efficacy of AST against multiple cervical cancer cell lines. Further, García-Quiroz et al. (2014) have shown *in vivo* effectiveness utilizing a combination of calcitriol and AST against breast cancer. AST is known to inhibit the Ether-á go-go-1 (Eag1) potassium channel (Garcia-Ferreiro et al. 2004). For example, Diaz et al. (2009) showed that Eag1 expression in numerous cancer cell types and reported that AST exposure could increase apoptosis in keratinocytes. These authors concluded that Eag1 was an early indicator of cell proliferation leading to malignancies and could be a therapeutic target for hyperproliferating cells.

The data presented herein suggests that AST has potential for *in vivo* activity and that it might be useful for augmenting current approaches to enhance therapeutic efficacy. Indeed, combination therapy has been suggested as a way that inducers of autophagic cell death may complement existing cancer therapies. For example, recently Peng et al (2008) reported that berberine, an isoquinoline alkaloid and inducer of autophagy in lung cancer cell lines, potentiates the anti-cancer effects of radiation. Moreover, these investigators showed this combination therapy to be effective in preclinical animal models. In the current study, the *in vivo* efficacy of AST against prostate cancer growth was determined using a xenograft transplantation model in nude mice. A significant growth inhibition of PC3 tumor cells in mice given daily oral doses of AST for 3 weeks was observed. This data, in combination with observations illustrated in Fig. 5, provide promise that AST has *in vivo* activity that might be useful for augmenting current therapeutic approaches to enhance therapeutic efficacy. Indeed, combination therapy has been suggested as a way that inhibitors of autophagy may complement existing cancer therapies (Livesey et al.

2009; Farrow et al. 2014). As noted previously, we have observed that AST potentiates cell killing in 22Rv1 prostate cancer cells exposed to 10 Gy radiation in combination with 4 μ M and 8 μ M AST (Table 1). These data demonstrate that modulation of autophagy can increase the efficiency of prostate cancer cell killing with established prostate cancer therapies.

New developments in the understanding of autophagy have led to the realization that cell death via autophagy represents a mechanism of cell death distinct from apoptosis which has been termed programmed cell death type II (Kondo & Kondo, 2006). The selective induction of cell death is a characteristic exploited for cancer chemotherapeutics. The process of autophagy clearly plays an important role in regulation of cancer development and progression and has been implicated as a factor contributing to the sensitivity of tumor cells to anticancer therapy (Kondo et al 2005; Bursch et al 1996; Shingu et al 2009). The identification of compounds that selectively kill cancer cells through induction of autophagy would significantly expand the therapeutic options for cancer treatments. Studies are currently underway to examine the interplay between AST-induced autophagy modulation and prostate cancer cell death.

Acknowledgements: Support for this study was provided by the University of New Mexico Cancer Center Focus-Interactive Group Award (TAT).

References

1. Altman BJ, Rathmell JC (2012) Metabolic stress in autophagy and cell death pathways. *Cold Spring Harb Perspect Biol.* 4:1-16 (a008763). doi: [10.1101/cshperspect.a008763](https://doi.org/10.1101/cshperspect.a008763)
2. Bursch W, Ellinger A, Kienzl H, Török L, Pandey S, Sikorska M, Walker R, Hermann RS (1996) Active cell death induced by the anti-estrogens tamoxifen and ICI 164 384 in human mammary carcinoma cells (MCF-7) in culture: the role of autophagy. *Carcinogenesis.* 17:1595-1607.
3. de Guadalupe Chávez-López M, Hernández-Gallegos E, Vázquez-Sánchez AY, Gariglio P, Camacho J (2014) Antiproliferative and proapoptotic effects of astemizole on cervical cancer cells. *Int J Gynecol Cancer.* 24:824-828. doi: [10.1097/IGC.0000000000000151](https://doi.org/10.1097/IGC.0000000000000151)
4. Díaz L, Ceja-Ochoa I, Restrepo-Angulo I, Larrea F, Avila-Chávez E, García-Becerra R, Borja-Cacho E, Barrera D, Ahumada E, Gariglio P, Alvarez-Rios E, Ocadiz-Delgado R, Garcia-Villa E, Hernández-Gallegos E, Camacho-Arroyo I, Morales A, Ordaz-Rosado D, García-Latorre E, Escamilla J, Sánchez-Peña LC, Saqui-Salces M, Gamboa-Dominguez A, Vera E, Uribe-Ramírez M, Murbartían J, Ortiz CS, Rivera-Guevara C, De Vizcaya-Ruiz A, Camacho J (2009) Estrogens and human papilloma virus oncogenes regulate human ether-à-go-go-1 potassium channel expression. *Cancer Res.* 69:3300-3307. doi: [10.1158/0008-5472.CAN-08-2036](https://doi.org/10.1158/0008-5472.CAN-08-2036)

5. Ellegaard AM, Dehlendorff C, Vind AC, Anand A, Cederkvist L, Petersen NH, Nylandsted J, Stenvang J, Mellemegaard A, Osterind K, Friis S, Jaattela M (2016) Repurposing cationic amphiphilic antihistamines for cancer treatment. *EBioMedicine*. 9:130-139. doi: [10.1016/j.ebiom.2016.06.013](https://doi.org/10.1016/j.ebiom.2016.06.013)
6. Farrow JM, Yang JC, Evans CP (2014) Autophagy as a modulator and target in prostate cancer. *Nat Rev Urol*. 11:508-516. doi: [10.1038/nrurol.2014.196](https://doi.org/10.1038/nrurol.2014.196)
7. García-Ferreiro RE, Kerschensteiner D, Major F, Monje F, Stühmer W, Pardo LA (2004) Mechanism of block of hEag1 K⁺ channels by imipramine and astemizole. *J Gen Physiol*. 124:301-317. doi: [10.1085/jgp.200409041](https://doi.org/10.1085/jgp.200409041)
8. Garcia-Quiroz J, Camacho J (2011) Astemizole: an old anti-histamine as a new promising anti-cancer drug. *Anticancer Agents Med Chem*. 11:307-314.
9. García-Quiroz J, García-Becerra R, Santos-Martínez N, Barrera D, Ordaz-Rosado D, Avila E, Halhali A, Villanueva O, Ibarra-Sánchez MJ, Esparza-López J, Gamboa-Domínguez A, Camacho J, Larrea F, Díaz L (2014) In vivo dual targeting of the oncogenic Ether-à-go-go-1 potassium channel by calcitriol and astemizole results in enhanced antineoplastic effects in breast tumors. *BMC Cancer*. 14:745. doi: [10.1186/1471-2407-14-745](https://doi.org/10.1186/1471-2407-14-745)

10. Haynes MK, Strouse JJ, Waller A, Leitao A, Curpan RF, Bologna C, Oprea TI, Prossnitz ER, Edwards BS, Sklar LA, Thompson TA (2009) Detection of intracellular granularity induction in prostate cancer cell lines by small molecules using the HyperCyt high-throughput flow cytometry system. *J Biomol Screen.* 14:596-609. doi: [10.1177/1087057109335671](https://doi.org/10.1177/1087057109335671)
11. Helsen C, Van den Broeck T, Voet A, Prekovic S, Van Poppel H, Joniau S, Claessens F (2014) Androgen receptor antagonists for prostate cancer therapy. *Endocr Relat Cancer.* 21:T105-118. doi: [10.1530/ERC-13-0545](https://doi.org/10.1530/ERC-13-0545)
12. Hu WW, Yang Y, Wang Z, Shen Z, Zhang XN, Wang GH, Chen Z (2012) H1-antihistamines induce vacuolization in astrocytes through macroautophagy. *Toxicol Appl Pharmacol.* 260:115-123. doi: [10.1016/j.taap.2012.01.020](https://doi.org/10.1016/j.taap.2012.01.020)
13. Jakhar R, Paul S, Bhardwai M, Kang SC (2016) Astemizole-histamine induces beclin-1-independent autophagy by targeting p53-dependent crosstalk between autophagy and apoptosis. *Cancer Lett.* 372:89-100. doi: [10.1016/j.canlet.2015.12.024](https://doi.org/10.1016/j.canlet.2015.12.024)
14. Kaini RR, Sillerud LO, Zhaorigetu S, Hu CA (2012) Autophagy regulates lipolysis and cell survival through lipid droplet degradation in androgen-sensitive prostate cancer cells. *Prostate.* 72:1412-1422. doi: [10.1002/pros.22489](https://doi.org/10.1002/pros.22489)

15. Kang C, You YJ, Avery L (2007) Dual roles of autophagy in the survival of *Caenorhabditis elegans* during starvation. *Genes Dev.* 21:2161-2171. doi: [10.1101/gad.1573107](https://doi.org/10.1101/gad.1573107)
16. Klionsky DJ, Abdelmohsen K, Abe A, Abedin MJ, Abeliovich H, Acevedo Arozena A, Adachi H, Adams CM, Adams PD, Adeli K, et al. (2016) Guidelines for the use and interpretation of assays for monitoring autophagy (3rd edition). *Autophagy* 12:1-222. doi: [10.1080/15548627.2015.1100356](https://doi.org/10.1080/15548627.2015.1100356)
17. Kondo Y, Kanzawa T, Sawaya R, Kondo S (2005) The role of autophagy in cancer development and response to therapy. *Nat Rev Cancer.* 5:726-734. doi: [10.1038/nrc1692](https://doi.org/10.1038/nrc1692)
18. Kondo Y, Kondo S. Autophagy and cancer therapy (2006) *Autophagy.* 2:85-90.
19. Kroemer G, Jäättelä M (2005) Lysosomes and autophagy in cell death control. *Nat Rev Cancer* 5:886-897. doi: [10.1038/nrc1738](https://doi.org/10.1038/nrc1738)
20. Kung CP, Budina A, Balaburski G, Bergenstock MK, Murphy M (2011) Autophagy in tumor suppression and cancer therapy. *Crit Rev Eukaryot Gene Expr.* 21:71-100.
21. Levine B, Klionsky DJ (2004) Development by self-digestion: molecular mechanisms and biological functions of autophagy. *Dev Cell* 6:463-477.

22. Livesey KM, Tang D, Zeh HJ, Lotze MT (2009) Autophagy inhibition in combination cancer treatment. *Curr Opin Investig Drugs*. 10:1269-1279.
23. Loos B, Engelbrecht AM (2009) Cell death: a dynamic response concept. *Autophagy* 5:590-603.
24. Nelson MP, Shacka JJ (2013) Autophagy modulation in disease therapy: where do we stand? *Curr Pathobiol Rep*. 1:239-245. doi: [10.1007/s40139-013-0032-9](https://doi.org/10.1007/s40139-013-0032-9)
25. Oprea TI, Bauman JE, Bologna CG, Buranda T, Chigaev A, Edwards BS, Jarvik JW, Gresham HD, Haynes MK, Hjelle B, Hromas R, Hudson L, MacKenzie DA, Muller CY, Reed JC, Simons PC, Smagley Y, Strouse J, Surviladze Z, Thompson TA, Ursu O, Waller A, Wandinger-Ness A, Winter SS, Wu Y, Young SM, Larson RS, Willman C, Sklar LA (2011) Drug repurposing from an academic perspective. *Drug Discov Today Ther Strateg*. 8:61-69. doi: [10.1016/j.ddstr.2011.10.002](https://doi.org/10.1016/j.ddstr.2011.10.002)
26. Peng PL, Kuo WH, Tseng HC, Chou FP (2008) Synergistic tumor-killing effect of radiation and berberine combined treatment in lung cancer: the contribution of autophagic cell death. *Int J Radiat Oncol Biol Phys*. 70:529-542. doi: [10.1016/j.ijrobp.2007.08.034](https://doi.org/10.1016/j.ijrobp.2007.08.034)

27. Pugh TJ, Nguyen BN, Kanke JE, Johnson JL, Hoffman KE (2013) Radiation therapy modalities for prostate cancer. *J Natl Compr Canc Netw*. 11:414-421.
28. Shingu T, Fujiwara K, Bögler O, Akiyama Y, Moritake K, Shinojima N, Tamada Y, Yokoyama T, Kondo S. Stage-specific effect of inhibition of autophagy on chemotherapy-induced cytotoxicity. *Autophagy*. 5:537-539.
29. Siegel RL, Miller KD, Jemal A (2017) Cancer Statistics, 2017. *CA Cancer J Clin*. 67:7-30. doi: [10.3322/caac.21387](https://doi.org/10.3322/caac.21387)
30. Van Limbergen J, Stevens C, Nimmo ER, Wilson DC, Satsangi J. Autophagy: from basic science to clinical application. *Mucosal Immunol*. 2:315-330. doi: [10.1038/mi.2009.20](https://doi.org/10.1038/mi.2009.20)
31. Wu WK, Coffelt SB, Cho CH, Wang XJ, Lee CW, Chan FK, Yu J, Sung JJ (2012) The autophagic paradox in cancer therapy. *Oncogene*. 31:939-953. doi: [10.1038/onc.2011.295](https://doi.org/10.1038/onc.2011.295).
32. Xie Z, Klionsky DJ (2007) Autophagosome formation: core machinery and adaptations. *Nat Cell Biol*. 9:1102-1109. doi: [10.1038/ncb1007-1102](https://doi.org/10.1038/ncb1007-1102)

33. Zhou S, Zhao L, Kuang M, Zhang B, Liang Z, Yi T, Wei Y, Zhao X (2012)
Autophagy in tumorigenesis and cancer therapy: Dr. Jekyll or Mr. Hyde? *Cancer
Lett.* 323:115-127. doi: [10.1016/j.canlet.2012.02.017](https://doi.org/10.1016/j.canlet.2012.02.017).

Figure Legends

Fig. 1. AST-induced changes in human prostate cancer cell line growth and viability. (A) Differences in AST dose-response for cell viability were determined for androgen-sensitive 22Rv1 and LNCaP human prostate cancer cell lines; and in the androgen-independent PC3 prostate cancer cell line, 48 h after AST treatment. AST induced a dose-dependent decrease in cell growth in the PC3 cell line (B) as well as the LNCaP cell line (C) 96 h after AST treatment. * $P < 0.05$ compared to control; # indicates significant cell death compared to control cells.

Fig. 2. Granularity analysis of PC3 human prostate cancer cells treated with AST. (A) Vehicle-treated control cells, low power; (B) cells treated with 10 μM AST; (C) higher power with 10 μM AST. Flow cytometric analysis of forward- (FSC-H) and side-scatter (SSC-H) changes in untreated (D) or 10 μM AST –treated PC3 prostate cancer cells (E). The R1 gate (i.e., red gate) was set to determine AST-induced changes in SSC as a measure of cellular granularity. (F) AST dose-response analysis of granularity as measured by changes in SSC. AST doses of 10 μM or greater produced significant PC3 cell death with lower levels of SSC compared to cells treated with 3 μM AST.

Fig. 3. Modulation of autophagy by AST in human prostate cancer cells. Control, vehicle-treated PC3 cells show low levels of cytoplasmic punctae (A), whereas cells treated with 10 μM AST for 24 hours produced notable punctae in PC3 cells expressing LC3-EGFP linked protein (B); arrows point to cells expressing pronounced punctae formation indicative of autophagy induction (B). Untreated PC3 cells stained with

acridine orange show low level staining (C), whereas PC3 cells treated with 10 μ M AST show significant acridine orange staining in acidic cytoplasmic vesicles. Arrows point to cells with pronounced acridine-orange-stained granules (orange-red; D). (A-D) Magnification 400 \times . (E) Immunoblot analysis for autophagy induction measured by LC3 lipidation. 22Rv1 prostate cancer cells were treated with 10 μ M AST for 6 hours. An increase LC3 lipidation by AST is indicative of autophagy modulation (E).

Fig. 4. Radiation and AST induced changes in PC3 prostate cancer cell viability and cellular fragmentation. (A) MTS cytotoxicity assay of AST and radiation induced cell death in PC3 cells (n=4; * P <0.05 compared to control). (B) Immunoblot analysis and quantification of LC3 II protein, a biomarker for the modulation of autophagy in PC3 cells treated with radiation with or without 8 μ M AST. (C) Cell fragmentation induced by AST and radiation treatment in PC3 cells measured by flow cytometry. (D) 10 μ M AST increased cellular fragmentation to 54.4 % (red arrow). (E) Fifteen μ M AST increased cell fragmentation to 76.0 % (red arrow). Cells were gated based on side-scatter (SSC) and forward-scatter (FSC) patterns. P1 = cell fragmentation gate showing back-ground levels (red arrow). P2 = non-fragmented % of PC3 cells (blue arrow). (F) Quantification of cellular fragmentation. Radiation and AST treatment significantly increased fragmentation (n=3; * P <0.05).

Table 1 Cell Death Response of AST Combined with Docetaxel or Radiation

% VIABILITY

Treatment	[5-fluorouracil (5-FU) + Mitomycin (M)]			
	0	2	4	8
Control	100.7 (7.2)	98.2 (4.0)	100.6 (1.2)	104.3 (1.4)
5-FU alone control	100.7 (1.2)	79.2 (4.1)	73.4 (4.0)	60.2 (1.2)
5-FU + radiation	100.3 (4.1)	65.4 (1.1)	62.1 (1.0)	52.2 (1.1)

* Viability to 5-FU (100 μg/ml) or radiation (20 Gy) alone was reported by the group before combination, n = 3.

† Viability to 5-FU treatment with combination therapy.

‡ Viability to radiation (20 Gy) with combination therapy.

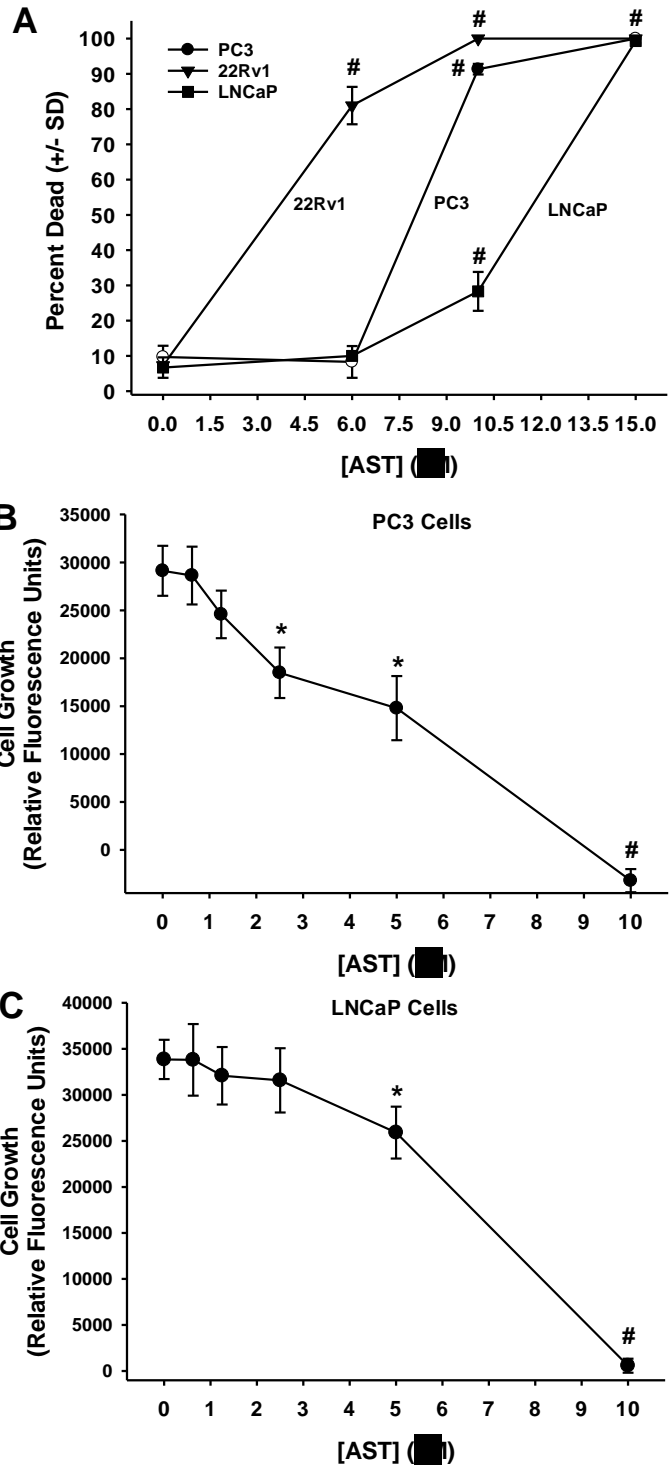


Figure 1.

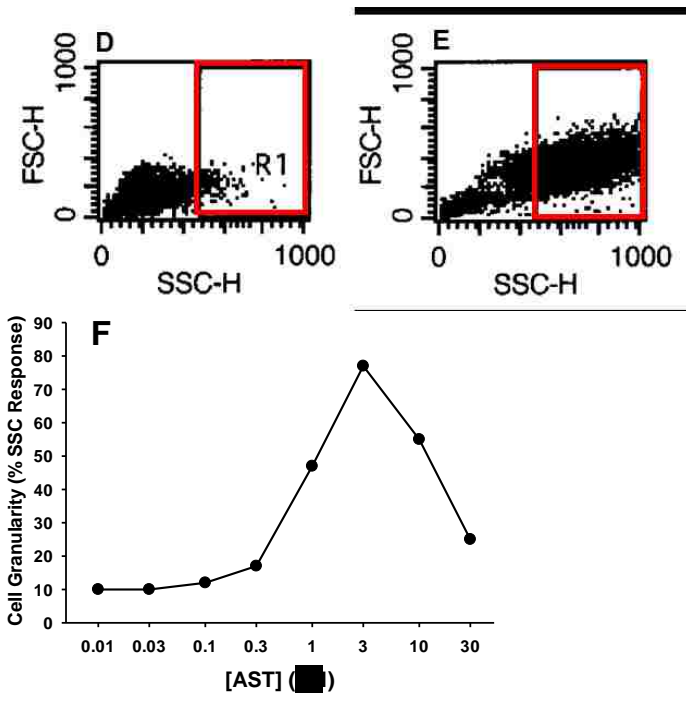
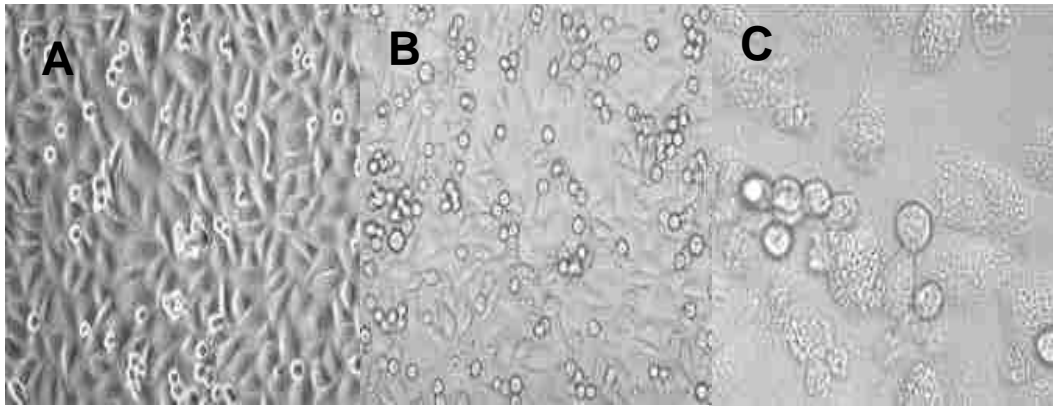


Figure 2.

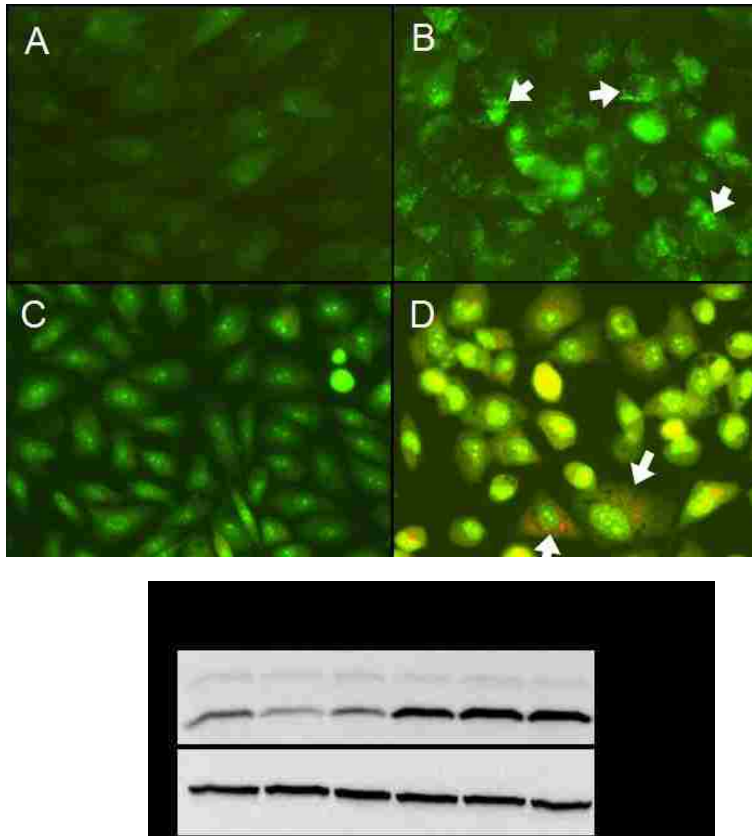


Figure 3.

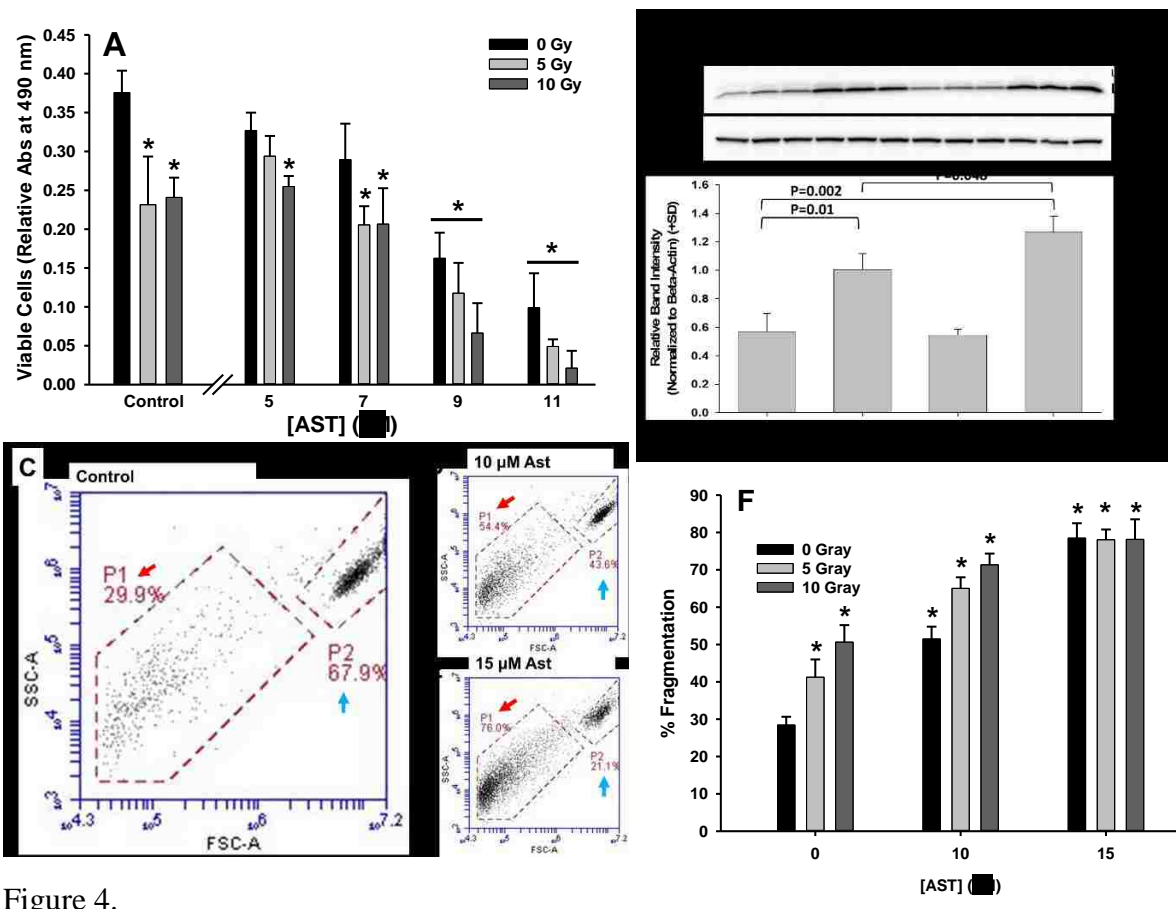


Figure 4.